Energy Conversion and Management: X 7 (2020) 100050

Contents lists available at ScienceDirect

Energy Conversion and Management: X

journal homepage: www.journals.elsevier.com/energy-conversion-and-management-x

Integration of gas switching combustion and membrane reactors for exceeding 50% efficiency in flexible IGCC plants with near-zero CO_2 emissions

Carlos Arnaiz del Pozo[a], Schalk Cloete[b,*], Paolo Chiesa[c], Ángel Jiménez Álvaro[a], Shahriar Amini[b]

[a] Universidad Politécnica de Madrid, Madrid, Spain
[b] SINTEF Industry, Trondheim, Norway
[c] Politecnico di Milano, Milan, Italy

ARTICLE INFO

Keywords:
CO_2 capture
Chemical looping combustion
Hydrogen membranes
Hydrogen
Flexibility
Integrated gasification combined cycle

ABSTRACT

Thermal power plants face substantial challenges to remain competitive in energy systems with high shares of variable renewables, especially inflexible integrated gasification combined cycles (IGCC). This study addresses this challenge through the integration of Gas Switching Combustion (GSC) and Membrane Assisted Water Gas Shift (MAWGS) reactors in an IGCC plant for flexible electricity and/or H_2 production with inherent CO_2 capture. When electricity prices are high, H_2 from the MAWGS reactor is used for added firing after the GSC reactors to reach the high turbine inlet temperature of the H-class gas turbine. In periods of low electricity prices, the turbine operates at 10% of its rated power to satisfy the internal electricity demand, while a large portion of the syngas heating value is extracted as H_2 in the MAWGS reactor and sold to the market. This product flexibility allows the inflexible process units such as gasification, gas treating, air separation unit and CO_2 compression, transport, and storage to operate continuously, while the plant supplies variable power output. Two configurations of the GSC-MAWGS plant are presented. The base configuration achieves 47.2% electric efficiency and 56.6% equivalent hydrogen production efficiency with 94.8–95.6% CO_2 capture. An advanced scheme using the GSC reduction gases for coal-water slurry preheating and pre-gasification reached an electric efficiency of 50.3%, hydrogen efficiency of 62.4%, and CO_2 capture ratio of 98.1–99.5%. The efficiency is 8.4%-points higher than the pre-combustion CO_2 capture benchmark and only 1.9%-points below the unabated IGCC benchmark.

1. Introduction

As highlighted by the Intergovernmental Panel on Climate Change [1], Carbon Capture and Storage (CCS) will play a vital role in reaching the climate change targets of restricting global warming to 1.5 °C above pre-industrial levels. Based on [2], CCS will be responsible for approximately 9% of the cumulative emissions reduction until 2050, amounting to approximately 2.8 billion tonnes per annum of CO_2 stored with around half of that amount originated in the power sector. Furthermore, CCS offers the possibility to balance the mitigation of carbonaceous emissions with economic growth. As pointed out in [3], the availability of low carbon emission energy solutions such as thermal power plants with CCS can result in electricity costs up to 62% lower than using renewables alone. Therefore, CCS, as a proven and well-understood technology, is pivotal to enable a transition to a low emissions economy for countries currently reliant on carbon-intensive electricity generation systems.

Amongst the different technologies available for carbon sequestration in thermal power plants, chemical looping combustion (CLC) proposed by Ishida et al. [4] promises high degrees of CO_2 capture and attractive economics [5]. This technology consists of carrying out the combustion of fuel by reducing a metallic oxygen carrier in a fuel reactor, which is later transported to an air reactor, subsequently reacting with oxygen and releasing heat utilized in a power cycle. Thus, an inherent CO_2 separation is achieved, minimizing the energy penalty of CO_2 capture relative to conventional abatement strategies [6]. However, progress on scale-up of dual interconnected fluidized bed reactors of gas-fuelled CLC systems at pressurized conditions has been slow [7]. High-pressure operation is a requisite for high power cycle efficiency. To overcome this problem, while ensuring high load flexibility of the power cycle, the gas switching reactor concept operating with fluidized beds was introduced in previous work by the authors [8]. This concept keeps the oxygen carrier in a single reactor where it is sequentially exposed to air and fuel streams through a valve switching mechanism,

* Corresponding author.
E-mail address: schalk.cloete@sintef.no (S. Cloete).

https://doi.org/10.1016/j.ecmx.2020.100050
Received 13 May 2020; Received in revised form 8 July 2020; Accepted 9 July 2020
Available online 18 July 2020

Nomenclature

Acronyms

ASU	Air Separation Unit
AGRU	Acid Gas Removal Unit
CCS	Carbon Capture Utilization & Storage
CGE	Cold Gas Efficiency
CLC	Chemical Looping Combustion
COT	Combustor Outlet Temperature
CSTR	Continuous Stirred Tank Reactor
GSC	Gas Switching Combustion
GT	Gas Turbine
HGCU	Hot Gas Clean Up
HSRG	Heat Recovery Steam Generator
HP	High Pressure
HTW	High Temperature Winkler
IGCC	Integrated Gasification Combined Cycle
IP	Intermediate Pressure
LP	Low Pressure
MAWGS	Membrane Assisted Water Gas Shift
MITA	Minimum Temperature Approach
PCB	Pulverized Coal Boilers
SEC	Syngas Effluent Cooler
TIT	Turbine Inlet Temperature
TOT	Turbine Outlet Temperature
VGV	Variable Guide Vane
VRE	Variable Renewable Energy
WGS	Water Gas Shift

List of Symbols

c_p	Specific heat capacity (J/mol.K)
d_t	Membrane tube diameter (m)
E_a	Activation Energy (J/mol)
h	Specific enthalpy (J/mol)
n	Total moles (mol)
f	Species molar flow (mol/s)
F	Total flow (mol/s)
K_{eq}	Equilibrium constant (-)
P	Pressure (bar)
r	Species reaction rate (mol/s)
R	Gas Constant (J/molK)
t	Time (s)
T	Temperature (K)
U	Heat transfer coefficient (W/m^{2}K)
y	Molar fraction (-)
z	Height (m)
ξ	Global reaction rate (mol/s)
ε	Voidage (-)
υ	Stoichiometric coefficient (-)
ϕ''	Molar flux (mol/m^{2}s)
ρ_s	Solids density (kg/m^3)
w_c	Catalyst weight fraction (-)
d_t	Tube diameter (m)

Subscripts/Superscripts

k	Component
i	Stream
r	Reaction
$^\circ$	Ambient/reference conditions
R	Retentate
P	Permeate

avoiding the need for solids circulation. A small decrease in capture ratio is observed resulting from the undesired mixing of outlet streams during valve switch from reduction to oxidation stage [9]. The thermodynamic efficiency of CCS plants based on GSC is noticeably hampered if the oxygen carrier material temperature limit is low [10]. Although several studies assume a maximum value of up to 1200 °C [11–13], it is still substantially below the firing temperatures achievable by modern gas turbine technologies [14]. Our previous work [13] showed that a significant efficiency benefit is attained when by-passing a portion of the syngas fuel to an extra combustor, which enables an increase in the turbine inlet temperature (TIT) values beyond CLC limits. This TIT increase can also be achieved using natural gas instead, raising the temperature of the oxidation stage outlet stream from the GSC cluster to the Combustor Outlet Temperature (COT) of the modern gas turbine. Nonetheless, a substantial reduction of the carbon capture rate resulted from either of these strategies.

From the variety of thermal power plants using solids fuels, Integrated Gasification Combined Cycles (IGCC) have the potential to reach the highest efficiencies, due to the high temperatures achieved through a combined (Brayton + Rankine) power cycle which lead to a higher Carnot efficiency relative to the standalone Rankine power cycle of Pulverized Coal Boilers (PCB). This effect is more marked as advanced gas turbine technologies with firing temperatures above 1500 °C are widely deployed, and operational difficulties are overcome. These advances result in efficiencies exceeding the most modern ultra-supercritical boilers [15], which require special materials (nickel-based alloys) that result in comparatively higher costs. Additionally, IGCC plants present the lowest environmental footprint due to the possibility of removing harmful contaminants concentrated in the small flow rate of syngas generated after gasification [16]. In parallel to this, the concentrated CO_2 at high pressure contained in the syngas allows for easier and less energy-intensive CO_2 capture compared to plants such as coal-fired boilers where post-combustion removal systems from the CO_2 diluted, low-pressure exhaust stream are applied. In particular, high-temperature syngas desulphurization or hot gas clean up (HGCU), appears to be a compelling technology to further boost IGCC power plant efficiencies [17], eliminating the energy penalty associated with large temperature swings of cooling syngas to ambient conditions for treating and subsequent reheating of the fuel before firing in a Gas Turbine (GT). Zinc Oxide (ZnO) sorbents show favourable thermodynamics to reduce sulphur components in the syngas to ppm levels [18] over a wide range of operating temperatures.

In addition to high efficiency, low cost, and low environmental impact, an increasingly important requirement of thermal power plants is the balancing of the fluctuating power output of cheap variable renewable energy (VRE) in the form of wind and solar power. The fluctuating generation profile of wind and solar is incompatible with baseload power generation, creating an optimal power mix composed of VRE backed up primarily by mid-load power plants that supply electricity during times of limited wind and sun [19]. The capital underutilization inherent to this power mix imposes substantial system-level costs, also known as profile costs [19]. These costs increase sharply with the capital cost of the underutilized capital, which is problematic for capital-intensive clean power plants such as nuclear, biomass, and CCS. For this reason, CCS and variable renewables are generally seen as competitors rather than complements [20].

Aside from the economic challenges related to the deployment of CCS plants as mid-load generators to balance VRE, significant technical constraints also exist. In particular, the IGCC power plants targeted in this study are highly inflexible due to the gasification train consisting of

several process units in series designed to operate in continuous full-load mode. In addition, intermittent CO_2 influxes into downstream CO_2 transport and storage infrastructure also poses technical challenges [21].

The original contribution of the present study is the development of a novel IGCC configuration that overcomes these technical and economic challenges related to CCS power plants in power systems with increasing shares of VRE. The key feature of this plant is the steady-state utilization of the gasification train and all equipment related to CO_2 compression, transport, and storage, despite flexible power production for balancing VRE. In this way, the coal-fired power plant proposed in this study will achieve similarly large system-level benefits to the natural gas-fired gas switching reforming plant for flexible power and hydrogen production previously evaluated by one of the authors [22]. In addition, the proposed power plant configuration facilitates added firing after the GSC reactors to maximize efficiency without compromising CO_2 avoidance.

The next section outlines the novel flexible power and hydrogen concept proposed in this study. Subsequently, the methodology for integrated reactor and power plant modelling is described, and the detailed flexible plant layout is provided together with suitable benchmark plants. Then, the technical performance of the proposed flexible GSC-IGCC power and hydrogen configuration is presented both in power and hydrogen production modes. Thermodynamic efficiencies and CO_2 emissions are benchmarked consistently against an unabated IGCC plant and a pre-combustion CO_2 capture IGCC plant, which utilize a modern H-class GT in the power cycle and HGCU for contaminant removal, as opposed to F-class turbines and cold gas clean-up used in prior studies with IGCC plants with and without CCS [16,23,24]. In addition, an advanced heat integration configuration is also investigated, enabling net electric efficiencies exceeding 50% with CO_2 capture above 98%, while preserving a high level of flexibility. Finally, the main technology gaps that need to be closed to realize the promising performance of the plants investigated in this study are discussed, and conclusions are drawn to guide future work.

2. Proposed power plant concept

A simplified layout of the flexible clean power and hydrogen plant proposed in this work is provided in Fig. 1. Relative to previous work on the GSC-IGCC power plant [13], the primary modification is the addition of a membrane-assisted water–gas shift (MAWGS) reactor [25]. This reactor separates out a fraction of the syngas heating value as pure hydrogen after the gas clean-up unit. The Pd-based membrane used in this work, with very high H_2 selectivity, is alloyed with other metals to avoid surface poisoning from CO and H_2O, and has a suitable operating window for temperatures resulting from HGCU [26]. Depending on the electricity price at the time, this hydrogen can then be used either for added firing after the GSC reactors for high efficiency power production or directly exported to the market (green diamond in Fig. 1). Other configurations, such as the three reactor chemical looping system [27], can also produce power and hydrogen, but do not offer the same level of flexibility.

When the plant is operating in hydrogen production mode, the pressure inside the membranes of the MAWGS reactor is reduced, and more steam is added to the syngas to maximize H_2 extraction. The gas turbine is ramped down to 10% of its nominal load with no added H_2 firing to enable power production from the heating value remaining in the low-grade syngas exiting the MAWGS reactor. Such a very low gas turbine load is possible because of the flameless combustion in the GSC reactors that does not introduce any NOx formation and incomplete fuel combustion issues at low turbine load.

In both these operating modes, the operation of the gasification train and the downstream CO_2 transport and storage infrastructure remains almost unchanged, avoiding the considerable technical and economic challenges with flexible CCS power production described earlier. It is also noted that a steady-state operating point anywhere between full power and full hydrogen mode would also be possible, resulting in combined power and hydrogen production.

A more advanced configuration of the plant shown in Fig. 1 is also investigated in this study where the hot GSC reduction outlet gases are used to evaporate and pre-gasify a coal slurry in a pre-gasification heat exchanger. The pre-gasified slurry (syngas with entrained coal particles) is then fed to a High Temperature Winkler (HTW) gasifier [28] at a temperature close to the gasifier operating temperature. This pre-gasification substantially reduces the heat demand in the gasifier, bringing a large increase in cold gas efficiency (CGE) and reduction in air separation unit (ASU) power consumption. The added complexity of this pre-gasification heat exchanger is to some extent mitigated by replacement of the lock hopper system for coal loading with simpler slurry pumps.

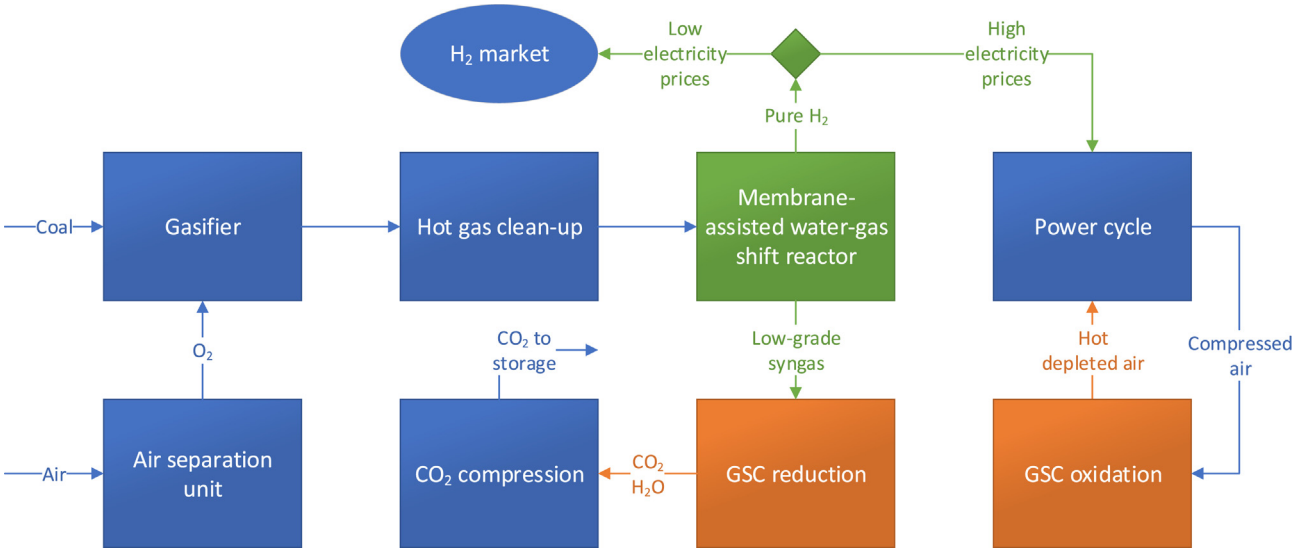

Fig. 1. Simplified schematic of the proposed flexible IGCC power plant layout.

3. Methodology

3.1. Model integration

The power plant models were elaborated in UniSim Design R451 [29] using the *Peng Robinson* equation of state for thermodynamic property calculation. The steam cycles employ *ASME steam tables*. GSC reactors were modelled in Scilab 6.0 [30], assuming the behaviour of a continuous stirred tank reactor (CSTR) to represent fluidized conditions, similarly to Cloete et al. [9]. The MAWGS reactor was also modelled in Scilab, assuming the behaviour of a plug flow reactor (PFR) with heat and mass diffusion effects. The kinetic rate of the WGS reaction was taken from Hla et al. [31], while a diffusion equation employed in Fernandez et al. [32] was used for H_2 permeation. The codes were two-way coupled to UniSim by means of a CAPE-OPEN unit operation. The GSC Scilab code solves the transient reactor profiles of temperature, flow, and composition and provides time-averaged values of temperatures and stage outlet mixing degrees to the stationary power plant model. The MAWGS Scilab model delivers the retentate and permeate reactor products provided a syngas stream. The gas turbine was modelled with the GS-code from the Energy Department of Politecnico di Milano, extensively used in the past to evaluate the performance of different power plants, e.g. [12,33,34], with the capability to accurately determine coolant flow requirements for different hot gas path conditions and compositions. The Patitug thermodynamic database from the Energy Department of the Universidad Politécnica de Madrid was used for property estimation within the Scilab codes assuming ideal gas behaviour, which is an acceptable simplification due to the high temperature and relatively low pressures encountered in these units. The change of fluid property package from one platform to another caused a relative mass & energy balance error below 0.1%. The solids properties used in the GSC reactors and HGCU model were predicted with correlations for enthalpy and specific heat obtained from data tables from [35,36].

The solving sequence to converge the MAWGS-GSC-GT loop was as follows: at a certain coal flow rate the syngas fraction to GSC and MAWGS was manipulated to reach simultaneusly the GSC averaged operating point and the nominal combustor temperature of the H-class turbine, for a given compressor air intake. Fuel stream compositions, temperature and relative flow to the cluster and extra firing chamber were delivered to the GS-code, which determined the GT net duty and actual air flow rate to the GSC cluster. Subsequenlty, the coal input in the Unisim flowsheet was manipulated to reach the same air flow to the GSC as predicted by the GT model. Since small variations in the MAWGS and GSC operating points occur, several iterations were carried out unitl both models predicted equal air flow rates to the cluster for the same fuel compositions. It is noted that the CAPE-OPEN unit operations allow to solve the MAWGS-GSC loop by exporting the product flows of each model to the stationary model, thus enabling a much faster convergence of the whole system.

3.2. Reactor modelling

3.2.1. Gas switching combustion (GSC) cluster

The transient behaviour of the GSC cluster was solved in the model built in Scilab analogously to previous studies [9,13] using a stiff ode function. A CSTR model is used to represent the fluidized bed, and complete fuel conversion is assumed, given the perfect mixing resulting from fluidization and the high NiO oxygen carrier reactivity [8]. Detailed computational fluid dynamics modeling of a large scale GSC reactor has shown these assumptions to be valid when high reactor temperatures are maintained, even for the natural ore, Ilmenite, that is much less reactive than NiO [37]. The molar species and energy balances solved in the code are represented by Eq. (1) and Eq. (2), respectively.

$$\frac{dn_k}{dt} = F_{in}y_{in,k} + F_{out}y_k + \sum_r \upsilon_{r,k}\xi_r \tag{1}$$

$$\sum_k n_k c_{p,k} \frac{dT}{dt} = -F_{in}\sum_k y_{in,k}(h_k - h_{in,k}) + \sum_k \sum_r \upsilon_{r,k}\xi_r h_k \tag{2}$$

These balances incorporate the primary hypothesis of the CSTR model, which assumes that the outlet flow of the reactor is at the same conditions (pressure, temperature, enthalpy, and composition) as the whole reactor volume. The oxygen carrier selected in this work was NiO, with the formulation taken from Abad et al. [38] and coherently with previous power generation assessments with CLC [39]. NiO is the most promising carrier due to its high oxygen carrier capacity and proven performance to fluidize at high temperatures [40]. The heterogeneous reactions considered, with a very fast reaction rate imposed by a τ value of 0.01 were:

$$CH_4 + 4NiO \rightarrow 4Ni + CO_2 + 2H_2O \quad r_{CH4} = \frac{1}{\tau} n_{CH_4} n_{NiO} \tag{3}$$

$$H_2 + NiO \rightarrow Ni + H_2O \quad r_{H2} = \frac{1}{\tau} n_{H_2} n_{NiO} \tag{4}$$

$$CO + NiO \rightarrow Ni + CO_2 \quad r_{CO} = \frac{1}{\tau} n_{CO} n_{NiO} \tag{5}$$

$$O_2 + 2Ni \rightarrow 2NiO \quad r_{O2} = \frac{1}{\tau} n_{O_2} n_{Ni} \tag{6}$$

To maintain a high average oxidation temperature, while achieving

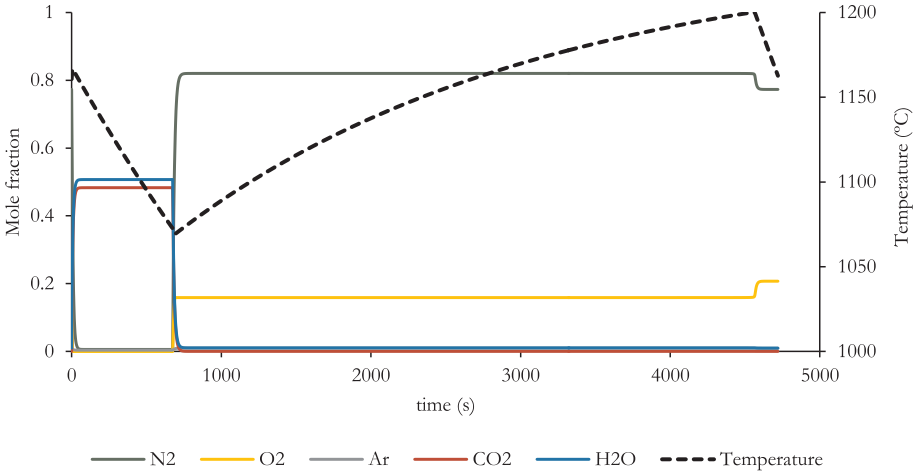

Fig. 2. Reactor temperature and composition profile during a reduction–oxidation cycle (case GSC-MAWGS with slurry pre-gasification in power mode).

a low degree of undesired outlet stream mixing during valve switch, the O_2 slip heat management strategy [37] was implemented. This reactor operation consists of a concentrated injection of air throughout the oxidation step that prevents all the oxygen from reacting, thus avoiding a sharp heat release at the beginning of the step. Furthermore, the delayed outlet valve switching strategy [9] was employed to maximize the cluster CO_2 capture in the reduction stage outlet stream. A fixed pressure drop of 0.5 bar was assumed in all the simulations

Fig. 2 illustrates the reactor behaviour for a GSC cluster of one of the presented power plant configurations. The reduction and oxidation step lengths were tuned to reach similar fluidization velocities of ~ 0.8 m/s using a cluster of 7 reactors 6 m in diameter and 12 m in height. The instantaneous outlet flows of the reactors in reduction and those in oxidation were mixed in two separate streams for feeding to the UniSim model, thus representing the cluster of dynamically operated GSC reactors as a steady state processing unit.

3.2.2. Membrane assisted water gas shift (MAWGS)

The MAWGS reactor was represented as a single reactor tube modelled in Scilab assuming a plug flow reactor, with mass (Eq. (8) & Eq. (9)) and energy (Eq. (10) & Eq. (11)) balances applied to each length differential of the tube to Retentate (R) and Permeate (P) sections, as shown in Fig. 3. The 1-D model is consistent with previous literature assessments of membrane technology integration in large scale IGCC power plants [41,42]. Further modelling assumptions of this unit can be found in Table 4 in the Appendix. The exothermic chemical reaction taking place in the tube length is shown in Eq. 7.

$$CO_2 + H_2O \rightarrow H_2 + CO_2 \qquad \Delta H_R^{\circ} = -40.6\ kJ/mol \tag{7}$$

$$\frac{\partial f_{k,R}}{\partial z} = r_k \rho_s w_c (1-\varepsilon)\frac{\pi d_t^2}{4} - \pi d_t \phi''_{k,R} \tag{8}$$

$$\frac{\partial f_{k,P}}{\partial z} = \pi d_t \phi''_{k,P} \tag{9}$$

$$\frac{\partial T_R}{\partial z} = \frac{-\sum h_{k,R}\frac{\partial f_{k,R}}{\partial z} + U\pi d_t (T_P - T_R)}{\sum f_{k,R} c_{pk,R}} \tag{10}$$

$$\frac{\partial T_P}{\partial z} = \frac{-\sum h_{k,P}\frac{\partial f_{k,P}}{\partial z} + U\pi d_t (T_R - T_P)}{\sum f_{k,P} c_{pk,P}} \tag{11}$$

The chemical reaction rate and diffusion flux across the membrane are obtained from the expressions given in Eq. (12) & Eq. (13). The power law coefficients and kinetic and equilibrium constant for the rate of reaction were taken from Hla et al. [31], while the parameters of the diffusion expression were assumed from Fernandez et al. [32]. Several experimental studies validate the assumption of infinite H_2 perm-selectivity through the membrane [43,44]

$$r_k = \upsilon_k k P_{CO}^a P_{CO_2}^b P_{H_2}^c P_{H_2O}^d \left(1 - \frac{P_{H_2} P_{CO_2}}{K_{eq} P_{CO} P_{H_2O}}\right) \tag{12}$$

$$\phi_k^{''} = \frac{P_0}{t_m} e^{\left(\frac{-E_a}{RT}\right)} \left(P_{k,R}^{0.74} - P_{k,P}^{0.74}\right) \tag{13}$$

Similarly to the GSC model, the MAWGS reactor model uses a stiff ordinary differential equation (ode) solver for temperatures and species molar flows. Fig. 4 illustrates the composition in the retentate profile and H_2 production in % of the total outlet flow across the permeate side of a membrane tube for one configuration of the power plants investigated. The WGS reaction proceeds rapidly to equilibrium at the start of the reactor length. In practice, it will be advisable to implement an adiabatic WGS reactor upstream to avoid sharp temperature gradients along the membranes, but this detail was neglected here for simplicity.

3.3. Power plant description

3.3.1. Unabated IGCC

A detailed schematic of the reference unabated IGCC power plant is given in Fig. 5. Stream data can be found in Table 7 in the Appendix for the case of a 2200 K SFT target.

Coal is gasified in an entrained flow gasifier, Shell type, operating at high temperature (> 1500 °C) where coal is fed via lock hoppers (using N_2 as transport gas) [23]. A gaseous quench with recirculated syngas cools the gasifier outlet to 900 °C, while a syngas effluent cooler (SEC), consisting of water economizer, steam evaporator and superheater, lowers the temperature further, producing a large amount of HP superheated steam at 450 °C. Oxygen with 95%mol purity is delivered to the gasifier by a high pressure pumped liquid oxygen air separation unit (HP PLOX-ASU), which is 50% integrated with the gas turbine compressor. Integration between the ASU & GT allows for operation closer to the design point of the compressor, compensating for the reduced air intake due to diluted syngas firing (which is a lower energy density fuel relative to natural gas). Since the ASU is operated at high pressure (10 bar approximately), N_2 with a purity above 98%mol is obtained at around 2.7 bar, which significantly reduces the compression duty of this stream required for subsequent syngas dilution. Higher integration of ASU and GT compressor is not recommended to avoid reliability and start-up issues [45].

After high-temperature solids removal in candle filters, the gasification island delivers syngas to a hot gas clean up unit (HGCU). This unit consists of interconnected fluidized beds with a Zinc Oxide (ZnO) desulphurization sorbent that is cyclically regenerated, following a similar approach for the modelling as Giuffrida et al. [17]. Experimental studies [46] reveal that complete H_2S adsorption assumption is acceptable, while additional sorbents are employed to remove other pollutants (NH_3, HCl, etc.) from the syngas stream [47]. The sorbent

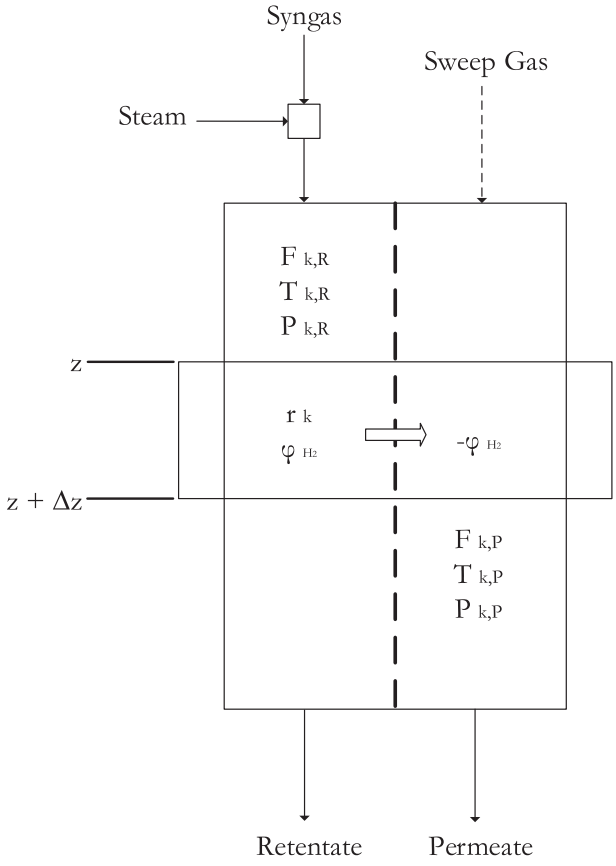

Fig. 3. Differential section of a membrane tube of the MAWGS reactor.

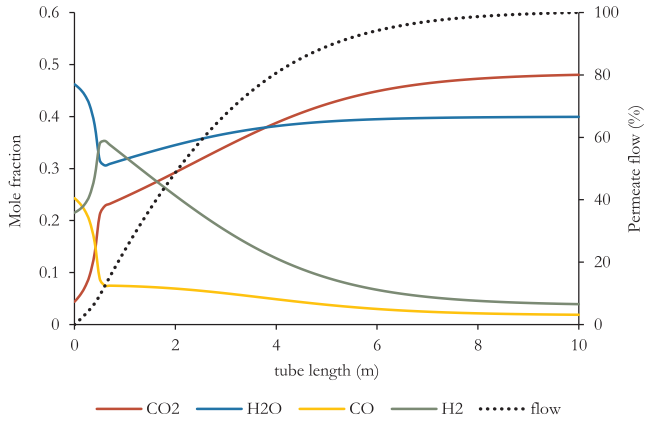

Fig. 4. Retentate composition profile and permeate flow in % for a tube length of the MAWGS reactor for a case designed for maximum hydrogen recovery.

regeneration is accomplished by using part of the N_2 from the ASU to provide a low O_2 concentrated stream (2%mol), reducing undesired sulphate formation in the regenerator bed. The outlet temperature of the syngas from the HGCU was fixed at 400 °C, in line with the operating temperatures of the candle filters, and to limit the temperature in the downstream membrane assisted water gas shift reactor (MAWGS) for the plants with gas switching combustion (GSC) discussed in the next section. Further increases of the clean-up temperature do not show great efficiency gains, as reported by Giuffrida et al. [48]. Since the adsorbent regeneration stream is already available from the ASU at slightly pressurized conditions, the compander unit used to deliver this stream to the pressurized regenerator and subsequently expand the off-gas product produces a net positive power output.

Premixed combustors used extensively with natural gas are challenging when dealing with syngas and H_2 fuels [49], resorting to diffusion flame combustors where the air is fed stoichiometrically to the fuel to maintain flame stability. Dilution is necessary to limit the adiabatic, stoichiometric flame temperature (SFT), which is directly related to NOx emissions [50]. Clean syngas is therefore subsequently diluted with the remaining N_2 from the ASU after a two-stage intercooled compressor to reach a final fuel pressure of 35 bar. However, to achieve sufficiently low SFT values, further dilution with steam from the bottoming cycle is still required as a consequence of feeding a high-temperature fuel (from HGCU) relative to the IGCC plants with low-temperature contaminant removal and syngas saturation [23]. Two SFT values of 2200 K and 2300 K are targeted to comply with acceptable ranges for IGCC plants [49].

The diluted fuel is fed to an H-class turbine with the specifications described in [51]. The combustor outlet temperature (COT) is adjusted to reach the same turbine outlet temperature (TOT) of 641 °C as the natural gas-fired reference, for all syngas fired cases. The turbine inlet temperature (TIT) is determined by the blade cooling flow model. It is assumed that, with Variable Guide Vane (VGV) closing and partial integration with the ASU, the compressor can run at the nominal pressure ratio and efficiency as when fired with natural gas. The GT exhaust is routed to a heat recovery steam generator (HSRG) with IP reheat in which steam is raised at three pressure levels. Since a substantial amount of HP steam is generated in the SEC, a large thermal duty is required for reheating, and the amount of steam produced in the IP drum is minimal. The HP evaporator of the HSRG is modelled as a once through boiler, while the condenser pressure was fixed at 4 kPa. Further details of the modelling assumptions can be found in the Appendix.

3.3.2. *Pre-combustion CO_2 capture IGCC*

A detailed schematic of this power plant model is shown in Fig. 6.

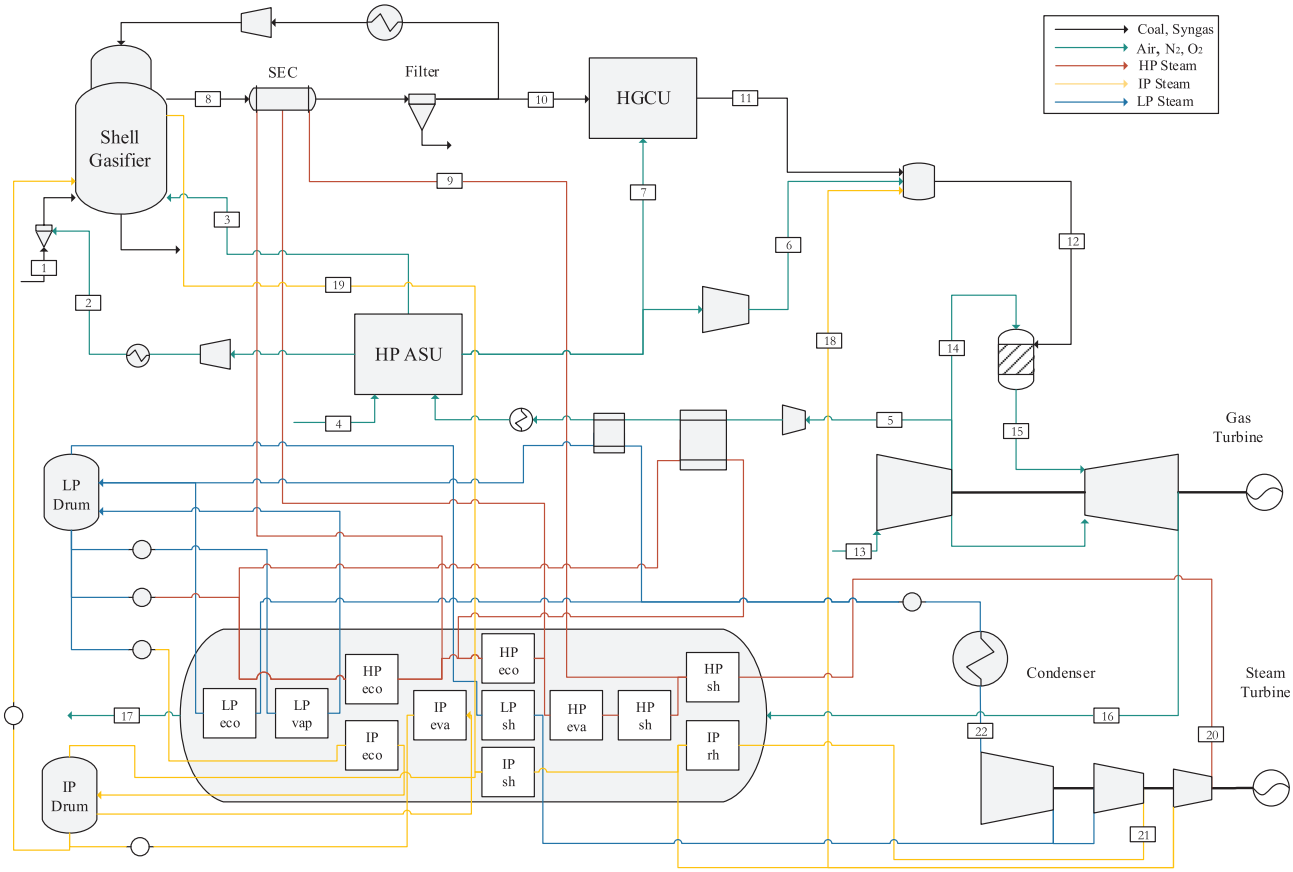

Fig. 5. Schematic of the Unabated IGCC power plant. Stream data can be found in Table 7 in the Appendix.

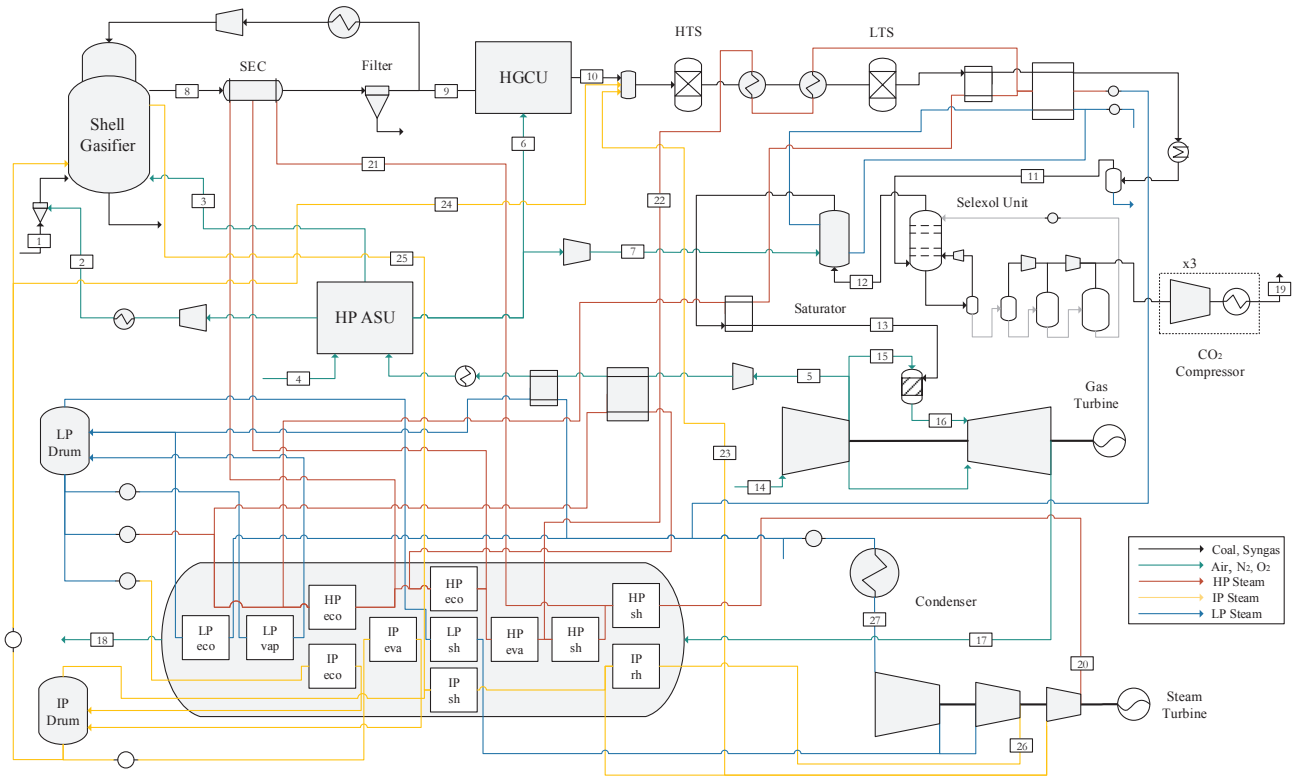

Fig. 6. Schematic of the pre-combustion CO_2 capture IGCC power plant. Stream data can be found in Table 8 the Appendix.

Detailed stream data for this power plant model is shown in Table 8 in the Appendix.

The reference plant with CCS consists of a pre-combustion CO_2 capture IGCC power plant extensively studied in previous works [23,24,52]. However, in this model, the benefits of HGCU treating are also incorporated. The gasification island is identical to the unabated IGCC plant, where an HP-ASU unit, which is 50% integrated with the GT compressor, delivers O_2 with 95% purity to a Shell gasifier. Coal is loaded with N_2 from the high-pressure column of the ASU. After syngas quench and cooling, the raw syngas is routed to the HGCU unit operating at 400 °C. After sulphur and contaminant removal, steam from the HP stage steam turbine outlet is added to reach the required H_2O/CO ratio for water gas shift conversion of 1.9. Because of the gas clean-up at elevated temperature, part of the H_2O is added as saturated water from the IP drum, tempering the mixture to reach the required High-Temperature Shift (HTS) inlet temperature of 300 °C. After WGS reaction in the adiabatic reactor bed, the syngas is cooled down to 200 °C, raising HP steam before it is fed to the Low-Temperature Shift (LTS). Equilibrium conversion is assumed in both beds, and the overall CO conversion is approximately 98%. A pressure drop of 1 bar per bed is specified. The shifted syngas is cooled down in a series of heat exchangers heating several water streams from the bottoming cycle, and further cooled down to ambient temperature. After water knock-out, the syngas is sent to an absorption column modelled with 10 equilibrium stages where Selexol removed approximately 94% of the CO_2. The use of a physical solvent is justified because of the high partial pressure of CO_2 achieved after the shift. Relative to previous studies [52], the Selexol absorption unit is simplified as there is no need in the present configuration for selective H_2S and CO_2 removal (due to HGCU). Instead, a single column line-up with solvent regeneration through pressure let-down is used, similarly to Arnaiz del Pozo et al. [53]. This sequential regeneration of the solvent at different pressures (7.5, 3, and 1.05 bar) reduces the CO_2 compression duty of the downstream 5-stage intercooled compressor. A CO_2 pump further increases the CO_2 stream pressure to 150 bar for transport and storage. Accounting for the CO_2 slip from the absorption unit and the unconverted CO from the WGS, the resulting plant capture ratio is approximately 91%.

The H_2 rich syngas is then mixed with N_2 from the ASU to reduce the flame temperature and avoid NOx formation. A small portion of the H_2 corresponding to 0.9% of the coal LHV is extracted for coal drying. Since the ASU delivers N_2 at 2.6 bar, all the available N_2 (minus the amount required for sorbent regeneration in the HGCU unit and for coal loading) is compressed to 35 bar in a two-stage intercooled compressor (with no aftercooler) and used for syngas dilution. The mixed stream is routed to a saturator unit integrated with the low-temperature heat recovery units of the shift conversion, increasing the moisture in the syngas, and then it is further heated to 220 °C. The syngas is subsequently fired in the H-class GT combustor. The N_2 and water added are sufficient to reach an SFT below the values targeted for the Unabated IGCC plant, due to the lower fuel temperature in this plant.

The bottoming cycle of the pre-combustion CO_2 capture IGCC plant with HGCU is identical to the Unabated IGCC reference plant, with a three pressure level with reheat HRSG. The steam cycle is consistently integrated with the steam demand and production of the WGS unit and gasification island.

Pre-combustion CO_2 capture IGCC plants also have the potential to alternate between H_2 and Power production [54,55]. However, these plants require the use of an additional Pressure Swing Adsorption unit (PSA) to purify the shifted syngas and would not be able to capitalize on the efficiency benefits of an integrated ASU. In the present work, however, this plant is designed exclusively for power generation as a benchmark of existing CCS technology.

3.3.3. GSC-MAWGS IGCC with reduction gases recuperator

A detailed schematic of this plant configuration is given in Fig. 7. Stream data for the power mode case are given in Table 9 in the Appendix.

The gasification island of the GSC-MAWGS IGCC plant is similar to the reference case, but analogously to Spallina et al. [12] coal is fed via

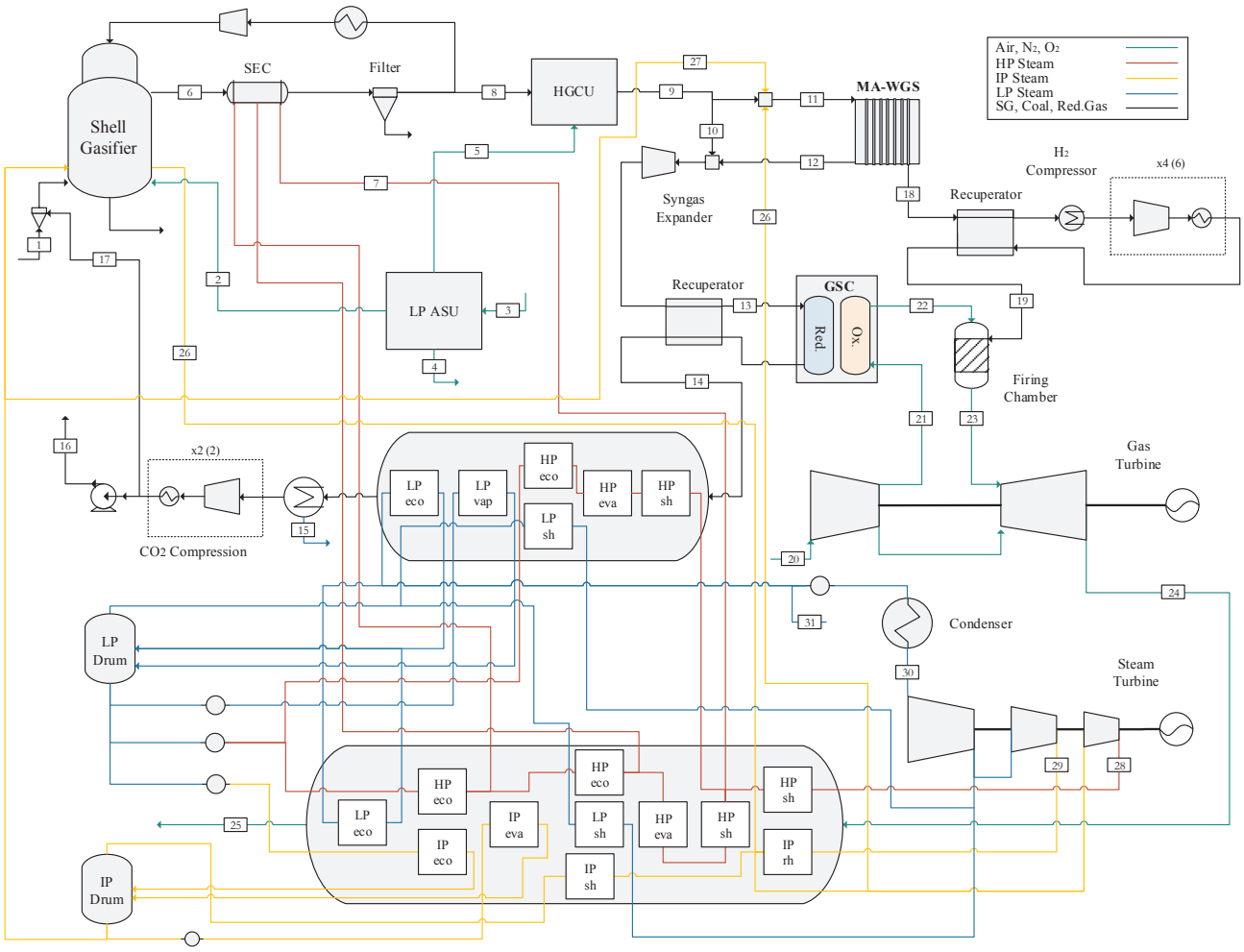

Fig. 7. Schematic of the GSC-MAWGS IGCC power plant with reduction gases recuperator. Stream data can be found in Table 9 in the Appendix.

lock hoppers with part of the captured CO_2 stream. The ASU consists of a standalone low-pressure cryogenic cycle, whose specific power consumption was taken from Spallina et al. [12], equal to 325 kWh/tonO_2. The LP-ASU configuration with no integration with GT compressor was selected to increase the plant flexibility in H_2 production operation mode, and because there is no need to dilute syngas with N_2. After hydrogen sulphide and other contaminants are removed in the HGCU unit, clean syngas is mixed with IP steam from the HP stage steam turbine outlet prior to the shift conversion. The ratio of steam to CO in the feed stream to the shift reactor was set to 1.9, to prevent catalyst carbiding [23]. A small portion of the H_2O added to the syngas stream consists of saturated IP water from the IP drum, cooling the feed stream to the shift reactor to the extent that the maximum temperature in the membrane (outlet) does not surpass 600 °C. Since it is not required to shift all the CO available in the syngas to produce enough H_2 to reach the desired combustor temperature, a split flow configuration was adopted, bypassing part of the syngas directly to the GSC cluster. In this way, the steam consumption from the bottoming cycle is reduced.

The MAWGS reactor consists of a reactor vessel with a total of 6000 membrane tubes of fixed length (10 m) and diameter (0.05 m). These tubes would cost approximately 47 M€ at \$5000/m^2 [56], which is estimated to be about 2.5% of the total plant cost based on an earlier economic assessment of a GSC-IGCC plant [57]. The shift reaction takes place in the reactor, diffusing the H_2 product across the membranes to the permeate side, thereby increasing the equilibrium conversion to the products (H_2) in the retentate. The H_2 production (permeate flow) is controlled by specifying the permeate membrane pressure and/or the split flow ratio between the syngas that is shifted and that which is directly fed to the GSC. With these operational handles, the relative heating value routed to GSC (retentate) or extra firing chamber (permeate) can be controlled.

When the plant is operated in power production mode, the membrane permeate pressure is set to approximately 2.8 bar, and around 60% of the syngas is routed to the MAWGS reactors. These values represent the optimal trade-off between the energy penalty associated with steam extraction when a higher fraction of syngas is routed to the MAWGS reactor and the H_2 recompression duty, which depends on the permeate pressure imposed. The fraction of the syngas heating value that is routed to the GSC reduction stage, together with the retentate flow, must ensure that the GSC oxidation and reduction outlet temperatures calculated by the transient cluster model are reached, whereas the H_2 produced in the permeate side allows the O_2 depleted air stream from the GSC to reach the COT of the GT. The H_2 obtained in the permeate side is cooled down in a recuperative heat exchanger and then recompressed to 35 bar (required fuel pressure in the GT combustor) in a 4 stage intercooled compressor and subsequently heated in the recuperator before being fed to the extra firing chamber. A minimum temperature approach (MITA) of 20 °C was assumed in the recuperator. The MAWGS retentate, consisting of a low heating value syngas with a large amount of water and CO_2 and the bypassed syngas, is mixed and expanded to the pressure ratio delivered by the GT air compressor in a syngas expander. The syngas is then heated up in a recuperative heat exchanger before entering the GSC, using the hot gases from the reduction stage outlet. A MITA of 30 °C, resulting in a heat exchanger effectiveness of approximately 93% was employed. Special materials will be required to manufacture the heat exchanger

[58] due to the elevated hot end temperatures. This recuperator ensures that most of the sensible heat in the syngas/reduction gases stream is effectively transferred to the air stream, which will produce electricity upon expansion in the turbine. The reduced gases recuperator outlet is routed to a heat recovery unit where steam is raised. The stream is further cooled to ambient temperature and, after water removal, the CO_2 is compressed and pumped to a delivery pressure of 150 bar. Since the GSC outlet pressure is preserved (minus heat recovery pressure losses), the recompression duty is small, and only two intercooled compression stages are (plus a supercritical CO_2 pump).

Hot compressed hydrogen is fed to the added combustor to increase the COT to 1648 °C. It is assumed that well-distributed injection of the hydrogen fuel into the hot depleted air stream for spontaneous combustion in excess air can limit NOx formation in a similar way as a premixed combustor [50]. This avoids the need for dilution with N_2 or steam that is required when using diffusive flame combustors to avoid large NOx emissions, such as in the unabated IGCC plants. After GT expansion, the exhaust air stream is sent to an HSRG with three pressure levels and IP reheat for extra power production in a steam turbine, similar to the reference IGCC plants.

In H_2 production mode, the membrane permeate pressure is reduced to 1.6 bar, and the fraction of syngas sent to the MAWGS reactor is increased to 81%. In this mode, the GT runs at 10% load at a significantly lower pressure ratio than the nominal case. The H_2 produced is cooled down, raising steam for the bottoming cycle and compressed in the pressure stages that were used for fuel compression in the power production mode, and further compressed in two subsequent intercooled stages to a final delivery pressure of 150 bar [59].

Since the air flow rate to the oxidation step of the GSC reactors is reduced substantially due to the part-load GT operation, a larger number of the reactors are used in reduction mode (3) to maintain similar fluidization velocities in each reactor. The total number of reactors and the dimensions remain the same as in the power mode.

The depleted air stream from the GSC is expanded in the GT without added H_2 firing at a TIT around 400 °C below the nominal value. The exhaust gas is used to raise steam in the HSRG for the bottoming cycle and to supply IP steam to the MAWGS reactor. The same steam turbine stage efficiencies were assumed as in the power mode in this assessment, acknowledging that appropriate technological and maintenance approaches must be taken to make bottoming cycles more flexible [60]. Regarding the heat recovery units, a conservative assumption was taken, and the heat exchanger elements were specified with the same approaches as in the power mode. The items that require a larger size in H_2 mode, such as the CO_2 compressor, H_2 compressor, and syngas expander (due to the lower pressure ratio of the GT and MAWGS permeate and H_2 delivery pressures) were redesigned to fit the process requirements, considering that, in a future economic assessment study, the largest unit in each of the two modes should be accounted for, to reflect the extra capital expenditure resulting from flexible H_2 and power production.

3.3.4. GSC-MAWGS IGCC with slurry Pre-gasifier

A detailed schematic of this plant configuration is given in Fig. 8, while stream data for the power mode case is shown in Table 10 in the Appendix.

As explained earlier, the main difference in this plant is the use of a

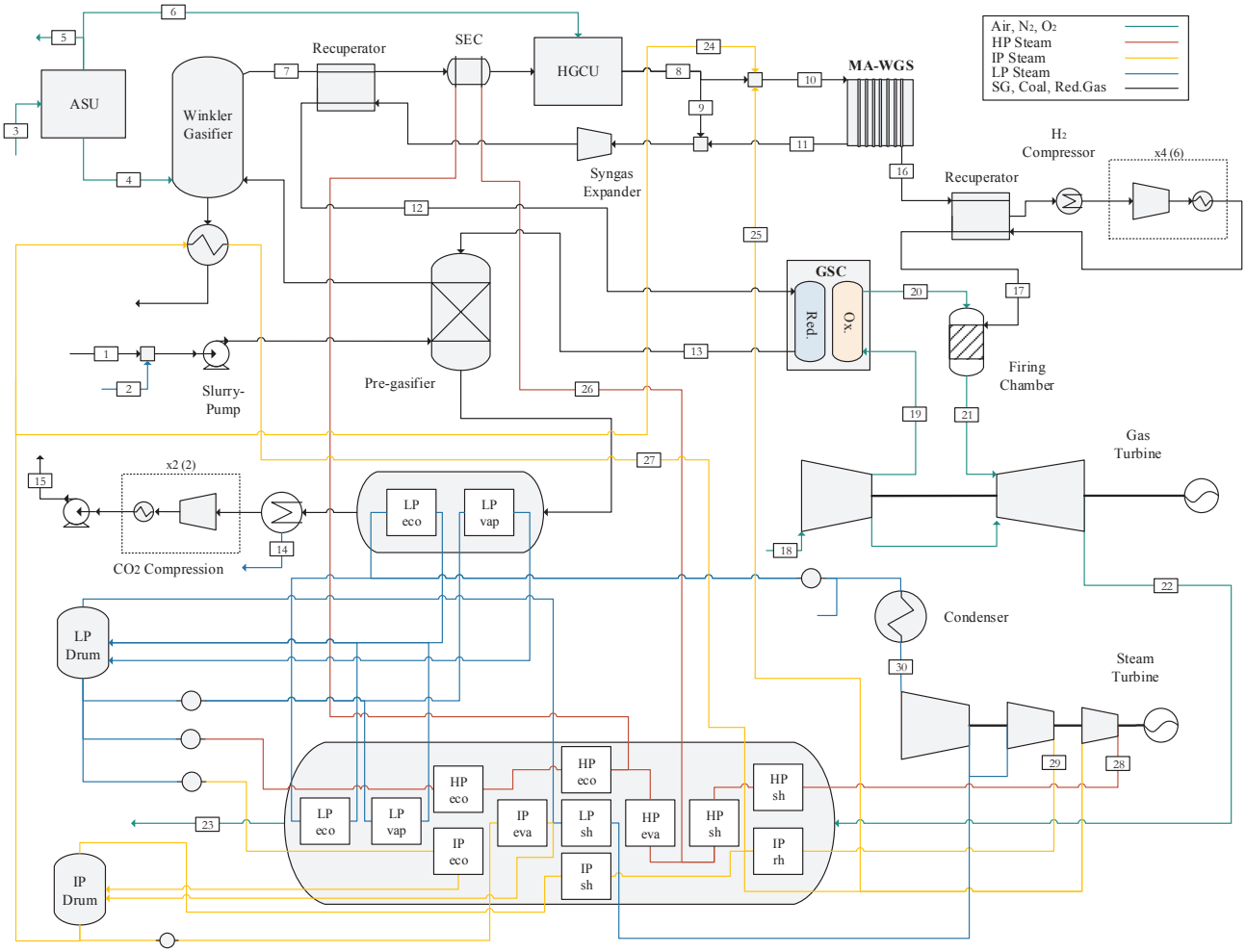

Fig. 8. Schematic of the GSC-MAWGS IGCC power plant with slurry pre-gasification. Stream data can be found in Table 10 in the Appendix.

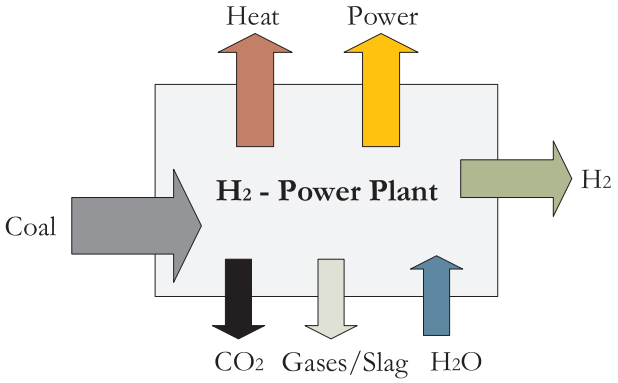

Fig. 9. Basic representation of a power plant system with H_2-power coproduction.

slurry pre-gasification heat exchanger to increase the CGE of the gasifier. The slurry pre-gasifier is modelled in two sections. The first is a heat exchange section where the water slurry is fully evaporated. The second section consists of the pre-gasification of coal, which is divided into 10 stages, each modelled as a gasifier unit with a proportional heat input provided by the GSC reduction outlet gases. An equal volume was specified to each gasifier stage section to ensure that, due to the endothermic gasification reactions taking place in the hot end, the temperature pinch occurs in the cold end of the pre-gasifier. In this way, the zone most prominent to fouling avoids a narrow temperature delta, allowing a high degree of heat extraction from the reduction gases stream.

The pre-gasifier outlet stream (syngas with entrained coal particles) is subsequently fed to a Winkler gasifier operating at 44 bar, and the O_2 demand from the ASU is manipulated to obtain a syngas stream at around 900 °C with a fixed carbon conversion reaching 97%. Because of the high-temperature pre-gasified feed and the circulating fluidized bed operation, this conversion value is achievable [61]. The operating pressure for this case was chosen to be the same as the Shell gasifier to maintain the same configuration for the MAWGS reactor. Although HTW gasifiers have up to now been demonstrated at around 30 bar, it is assumed that the scale up to a higher operating pressure is feasible due to the replacement of the dry feeding system with a slurry pump. Furthermore, the operating flexibility and fuel versatility of the HTW fluidized bed gasification will be advantageous for the pre-gasified slurry feed relative to an entrained flow gasifier.

The syngas produced in the HTW gasifier is routed to a recuperator and then to a small syngas cooler, which raises some HP steam, cooling it down prior to the HGCU. This recuperator, similar to the concept presented by Hack et al. [62], is suitable for a syngas produced in an HTW gasifier because the low operating temperature eliminates the need of any gas quench and therefore no syngas recirculation loops are present, resulting in an improved temperature profile relative to HP steam generation. The desulphurization temperature was fixed at 400 °C, as in the previous cases. Approximately 63% of the syngas is fed to the MAWGS reactor after the addition of IP steam/water. The retentate stream, together with the fraction of syngas bypassed directly to the GSC, is expanded in a syngas turbine and later routed to the recuperator, which operates with a MITA of 30 °C, exchanging heat with the syngas gasifier outlet. The heated fuel is then fed to the GSC reduction stage, heating the air stream delivered by the GT compressor to the GSC oxidation stage outlet temperature. The GSC reduction step outlet gases are fed to the pre-gasifier to heat the coal water slurry, operating with a temperature approach of 30 °C in the cold end of the exchanger. The cooled GSC reduction outlet stream is routed to a heat recovery unit consisting of an LP economizer and evaporator, which efficiently retrieves the condensation enthalpy of water present in this stream, generating LP steam for the bottoming cycle before being sent to the CO_2 compression section. The depleted air stream from the GSC is upgraded in the added combustor and expanded in the GT in the same way as described earlier.

In H_2 production mode, the GT runs at part load with a normalized output of 10%, as described before. In this case, since the MAWGS retentate stream contains a substantial heating value due to the presence of methane, a smaller fraction of the clean syngas after desulphurization must be routed directly to the GSC (around 10%). The high fraction of methane in the retentate makes the GSC reduction reactions more endothermic, reducing the reduction step outlet temperature relative to power mode operation. This results in less heat transfer in the pre-gasifier to the coal water slurry in the hot end of the exchanger, slightly increasing the O_2 demand from the ASU and reducing the CGE by around 2%-points relative to the power mode. Nonetheless, the large amount of heating value preserved in the syngas due to the high CGE results in a comparatively more attractive H_2 production efficiency. Analogously to the case with reduction gases recuperator, the H_2 is cooled down, raising HP steam and the compressed in a 6 stage intercooled compressor to 150 bar.

3.4. Key performance indicators

A simplified representation of the power plant system is provided in Fig. 9. The plant transforms the chemical energy of a coal fuel into H_2 and/or electricity. A series of by-product energy (heat released to ambient) and material streams (captured CO_2, exhaust air, gasifier slag etc.) are also plant outputs. Because of the large steam requirement in the WGS unit, a substantial amount of water make-up must be reintroduced into the steam cycle.

The definition of plant thermal efficiency is straightforward when the plant runs exclusively in power production mode (Eq. (14)). However, if H_2 is produced as well, two different hydrogen production efficiencies are calculated, without accounting (Eq. (15)) and with accounting (Eq. (16)) for the net power production of the plant. In Eq. (16), the reference plant efficiency is used, i.e. $\eta_{ref} = 0.516$, corresponding to the unabated IGCC plant with SFT of 2200 K.

$$\eta_t^{w} = \frac{\dot{W}_{net}}{\dot{m}_{coal} LHV_{coal}} [\%] \tag{14}$$

$$\eta_t^{H_2} = \frac{\dot{m}_{H_2} LHV_{H_2}}{\dot{m}_{coal} LHV_{coal}} [\%] \tag{15}$$

$$\eta_{t,eq}^{H_2} = \frac{\dot{m}_{H_2} LHV_{H_2}}{\dot{m}_{coal} LHV_{coal} - \frac{\dot{W}_{net}}{\eta_{ref}}} [\%] \tag{16}$$

Since the reference power plant was modelled only for electricity production, the CO_2 avoidance (Eq. (17)) and specific primary energy consumption for CO_2 avoided (SPECCA) (Eq. (18)) are quantified for the GSC plants only in power mode operation.

$$A_{co_2} = \frac{E_{CO_2,Ref} - E_{CO_2,CCS}}{E_{CO_2 Ref}} [\%] \tag{17}$$

$$SPECCA = 3600 \frac{\frac{1}{\eta_{t,CCS}} - \frac{1}{\eta_{t,Ref}}}{E_{CO_2,Ref} - E_{CO_2,CCS}} \left[\frac{MJ_{th}}{kgCO_2} \right] \tag{18}$$

Finally, the water consumption (dedicated to H_2 generation and syngas dilution for the unabated plant and the schemes with CCS, respectively) per unit of thermal input is also quantified (Eq. (19)).

$$wc = \frac{\dot{m}_{H_2O}^{make-up}}{\dot{m}_{coal} LHV_{coal}} \left[\frac{kg_{H_2O}}{GJ_{th}} \right] \tag{19}$$

4. Results and discussion

In this section, a detailed discussion of the power plant results for

the reference IGCC models and the configurations with GSC cluster and MAWGS reactor, for power and H_2 production modes, is given. Firstly, the power breakdown and key performance indicators for each case are provided, after which a more in-depth analysis of the GSC cluster, MAWGS reactors, GT integration, and pre-gasifier operation is presented. Finally, the key technology gaps that must be overcome to deploy these IGCC concepts are discussed.

4.1. Energy breakdown and CO_2 emissions performance

The different power plant model results from an energy and CO_2 emissions perspective are provided in Table 1, for power and H_2 production operating modes:

When analyzing the results from the benchmark unabated IGCC cases, a substantial efficiency enhancement with respect to past studies of IGCC plants without CCS is observed. This is partly due to the use of a highly efficient H-class gas turbine and higher steam temperatures in the bottoming cycle. Furthermore, it is also due to the added efficiency benefits of HGCU, which amounts to up to 2%-points of efficiency [17]. A large GT duty is obtained in this plant because of the large flow rate of fuel, which reduces the compressor air intake with respect to a natural gas-fired case and, consequently, the compression duty requirements. When looking at the influence of a lower SFT through a higher degree of dilution with steam, the power obtained in the topping cycle is higher for a lower SFT value, while the bottoming cycle output decreases because of the larger IP steam extraction. The results show a decrease of around 0.6%-points efficiency per 100 °C lower SFT.

On the other hand, when looking at the pre-combustion CO_2 capture IGCC plant, the energy penalty associated with CCS amounts to 9.7%-points. The benefits of HGCU for this plant are, to an extent, curtailed by the fact that shifted syngas cooling to ambient temperatures for CO_2 removal must still be done. Nonetheless, some IP steam savings are attained as the required steam/CO ratio in the HTS can be reached by addition of IP water (to quench the high-temperature clean syngas from the HGCU), which is less energy demanding to produce. Similarly, the removal of the sulphur compounds prior to the shift conversion simplifies the Selexol absorption train, resulting in a comparatively lower auxiliary consumption than schemes with syngas scrubbing and sour shift [23], as a lower solvent circulation rate is achieved and no LP steam is required for regeneration in the H_2S stripper unit. Around 9% of the CO_2 generated in this plant is emitted (originating primarily from the CO slip of the WGS unit and the CO_2 not captured in the Selexol plant). Because of the lower efficiency resulting from CCS, using the same GT, around 17% higher heat input (coal) must be fed to the plant, delivering approximately 5% lower electricity output. This results in a carbon avoidance of around 2%-points below the capture rate of the plant.

When comparing the unabated IGCC power plant against the GSC-MAWGS IGCC with reduction gases recuperator, the energy penalty of CO_2 capture results in only 4.4%-points. Since O_2 from the air stream is withdrawn in the GSC cluster, and the fuel input only consists of a small H_2 flow rate, the net turbine output is smaller than in the syngas fired cases. As only a small amount of fuel is added to the hot gas, the compressor operates at the nominal air flow intake with a slightly lower pressure ratio. Furthermore, substantial auxiliary power consumption is needed for H_2 compression.

A key feature to mention about the GSC-MAWGS plant is that the large energy penalty encountered by the pre-combustion CO_2 capture IGCC plant to produce an H_2 fuel is to a great extent avoided:

- Since only a fraction of the syngas is required to produce H_2 to reach COT from the GSC oxidation outlet, the steam extraction from the

Table 1
Power plant results. Negative values imply energy consumption.

Item	Unabated IGCC		Pre-combustion CO_2 Capture IGCC	GSC-MAWGS IGCC with reduction gases recuperator		GSC-MAWGS IGCCwith slurry pre-gasifier	
Design Mode	*SFT 2200 K*	*SFT 2300 K*	*SFT 2110 K*	*Power*	*H_2*	*Power*	*H_2*
Coal Input (MW)	1534.1	1525.3	1794.9	1487.0	1487.0	1224.0	1224.0
GT Net (MW)	561.6	546.4	585.3	475.5	29.1	466.0	22.3
ST Net (MW)	332.7	351.8	347.3	328.3	158.2	205.0	56.2
Air /Syngas Expander (MW)	15.5	15.4	18.1	17.8	57.5	12.5	40.3
GT Aux. (MW)	−2.2	−2.2	−2.2	−2.2	−2.2	−2.2	−2.2
ASU (MW)	−47.4	−47.1	−55.5	−58.6	−58.6	−20.3	−24.0
N_2 Compression (MW)	−47.4	−47.2	−61.1	0	0	0	0
Syngas Recycle Compressor (MW)	−2.4	−2.3	−2.8	−1.9	−1.9	0	0
Coal Milling (MW)	−3.1	−3.0	−3.6	−3.0	−3.0	−2.4	−2.4
Ash Handling (MW)	−0.9	−0.9	−1.0	−0.9	−0.9	−0.8	−0.8
HGCU Aux. (MW)	−1.8	−1.8	−2.1	−1.7	−1.7	−1.4	−1.4
Compander (MW)	4.1	4.0	4.7	−0.4	−0.4	−0.4	−0.4
CO_2 Compression (MW)	0	0	−40.7	−18.7	−40.15	−11.6	−25.3
H_2 Compression (MW)	0	0	0	−19.2	−52.4	−19.6	−56.2
Selexol Unit (MW)	0	0	−20.7	0	0	0	0
Water Pumps (MW)	−6.3	−6.1	−7.4	−6.9	−4.8	−4.3	−2.5
Heat Rejection Aux. (MW)	−3.5	−3.8	−3.9	−3.8	−2.6	−2.8	−1.4
Total Condenser Duty (MW)	435.0	470.7	492.0	479.3	323.2	354.7	175.6
Balance of Plant (MW)	−2.4	−2.3	−2.7	−2.2	−2.2	−1.8	−1.8
Gross Plant (MW)	913.8	917.6	955.5	821.4	244.2	683.4	118.4
Net Plant (MW)	792.1	796.3	751.8	702.0	73.5	615.8	0.0
Total H_2 LHV (MW)	–	–	–	–	761.3	–	764.0
Gross Electric Efficiency (%)	59.6	60.2	53.2	55.2	16.4	55.8	9.7
η_t^w(%)	51.6	52.2	41.9	47.2	4.9	50.3	0.0
$\eta_t^{H_2}$(%)	–	–	–	–	51.2	–	62.4
$\eta_{t,eq}^{H_2}$(%)	–	–	–	–	56.6	–	62.4
E_{co_2}($kgCO_2/MWh_{H2+el.}$)	670.9	663.6	70.6	38.4	26.9	13.2	2.5
CC (%)	0	0	91.5	94.8	95.6	98.1	99.5
CA (%)	0	1.0	89.5	94.3	–	98.0	–
SPECCA ($MJ/kgCO_2$)	–	–	2.70	1.05	–	0.28	–
wc (kgH_2O/GJ_{th})	18.7	5.4	35.3	8.7	20.8	13.7	30.0

bottoming cycle is greatly reduced. For the pre-combustion plant, the syngas stream must be entirely shifted, needing much more steam.

- By using the recuperator and the syngas expander, the heat released in the WGS reaction is converted to power at a high efficiency. In the pre-combustion plant, the shifted syngas must be cooled to ambient temperatures, condensing most of the water for CO_2 removal through absorption, retrieving a small portion of the heat of reaction as HP steam.
- The pre-combustion plant recovers CO_2 at relatively low pressures and carries out the compression in 5 intercooled stages, while the pressurized reduction gases stream present in the GSC concepts allows to reduce the compression train size and associated auxiliary consumption quite significantly.

From a CO_2 emissions perspective, this plant achieves 3.8%-points higher capture than the pre-combustion CO_2 capture plant, with a 1.6 MJ/kgCO_2 lower SPECCA index and a CO_2 avoidance, which is around 5%-points higher.

When operating in H_2 production mode, the minimum load imposed by the GT results in a H_2 equivalent efficiency slightly below the literature values for pre-combustion CO_2 capture plants designed for low electricity production [55]. However, the range in which this plant can operate flexibly between H_2 and power production is much wider than for the plants in the aforementioned study (with *ad hoc* power cycles for different degrees of electricity outputs) as the GT can be ramped up safely from 10 to 100% power load. Furthermore, the high efficiency at which electricity is produced in the current reference plant tends to comparatively decrease the equivalent H_2 efficiency (Eq. (16)). If the pre-combustion CO_2 capture plant reference efficiency was used to calculate equivalent efficiency in Eq. (16), the resulting value would rise to 58.0%.

When looking at the GSC-MAWGS IGCC plant with slurry pre-gasification, it can be seen that the energy penalty is reduced to only 1.3%-points, reaching a capture rated above 98% due to the elimination of coal drying requirements and CO_2 lock hopper venting of the Shell gasifier. This results in a carbon avoidance that is 8.5%-points above the reference pre-combustion plant and a minimal SPECCA Index.

In terms of H_2 production equivalent efficiency, this configuration clearly surpasses the case with the reduction gases recuperator by approximately 6%-points. Interestingly, all the heat duty invested in 10% load GT operation is sufficient to satisfy the internal electricity demand of the plant, with a negligible net power output.

Finally, it can be mentioned that the process water make up required due to the shift conversion/syngas dilution units for these novel plants is also substantially lower than for the pre-combustion benchmark, mainly due to the large water retrieval in the reduction gases condenser.

4.2. Power plant system analysis

In order to fully comprehend how these efficiency benefits arise, a more in-depth analysis of the heating value distribution for the plants with GSC and MAWGS reactors is performed.

For the case with slurry pre-gasification, the hot feed to the gasifier results in a CGE of around 100% (effectively retaining all the coal heating value in the syngas) while substantially reducing the O_2 requirement from the ASU. This appealing result is due to the use of heat in the GSC reduction outlet gases to displace fuel combustion with O_2 in the gasifier. On the other hand, for the plant with reduction gases recuperator, only approximately 80% of the fuel heat input is preserved in the syngas that is distributed in between the GSC cluster and the membrane reactor, because of the lower CGE attainable in the dry-fed entrained flow Shell gasifier. The remaining heat is downgraded to HP steam in the SEC, which can only be utilized in the bottoming cycle for electricity production. This explains the large difference in H_2 production efficiency that is obtained between the models, as depicted in Fig. 10.

Alongside this, an illustrative heat-temperature profile of the pre-gasification unit is provided in Fig. 11. The effect of endothermic gasification reactions prevents a temperature pinch in the hot end of the exchanger, thereby extracting more heat from the reduction gases stream.

Thus, the water evaporation and heating in the slurry can be done directly with low-grade heat as the temperature profile of the coal-water slurry conveniently matches the cooling curve of the reduced gases stream. The higher temperature of the coal slurry fed to the HTW after the pre-gasifier results in a lower gasifier volume and a smaller oxidant stream required, and consequently a substantially smaller and ASU, that ultimately leads to a lower specific plant cost.

It should be noted that, due to the high operating pressure and low temperature of gasification, the syngas obtained in the models has a high methane fraction (around 7.3%mol), which represents approximately 22% of the coal LHV. These values are consistent with the trends reported in Higman [61] for similar operating conditions. Although this species cannot be effectively transformed to H_2 in the MAWGS reactor,

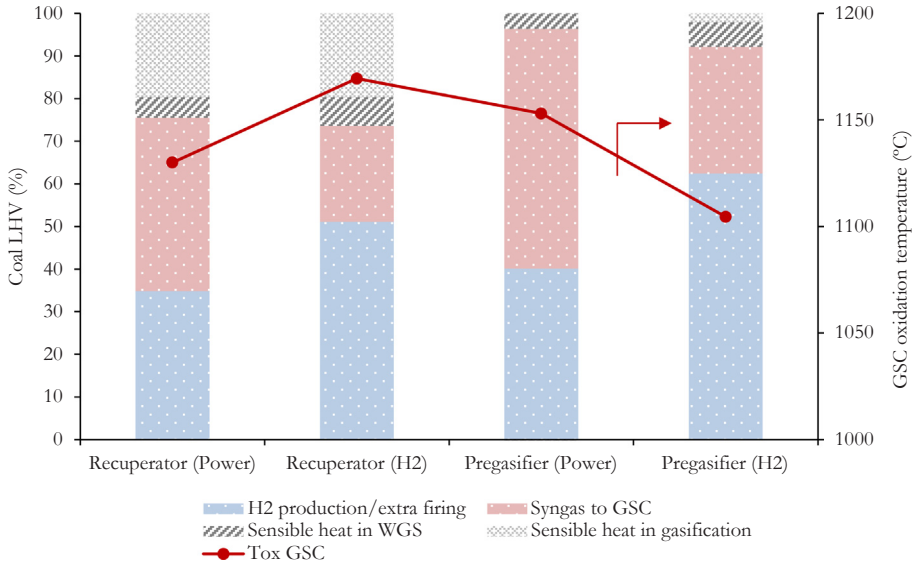

Fig. 10. Syngas after HGCU heating value distribution as coal LHV % for the different power plants with GSC-MAWGS.

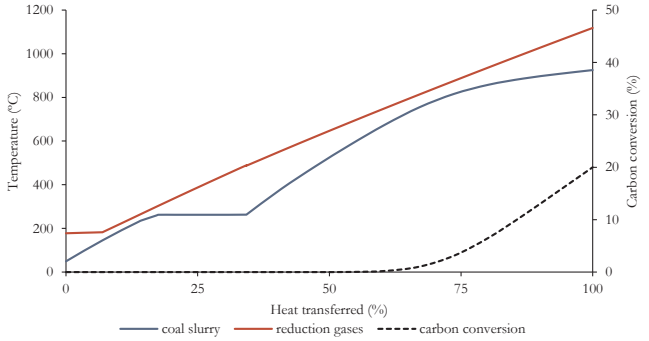

Fig. 11. Pre-gasifier temperature profile for the GSC-MAWGS IGCC plant in power production mode.

as the steam reforming equilibrium is inhibited at the reactor temperature [63], the presence of this high heating value component in the fuel allows to reach the required heat rate for 10% GT output operation in H_2 mode bypassing a smaller portion of syngas to the GSC. Together with the higher CGE attained in the HTW gasifier, the net overall effect is an increase of the H_2 production efficiency observed in Fig. 10, comparatively to the case with Shell gasification.

4.3. Key technology gaps

The realization of the promising results reported in this study requires further demonstration and scale-up of several process components. Four key technology gaps and associated risk mitigation strategies are briefly discussed below, in addition to potential challenges with flexible operation.

GSC reactors. Due to the simple standalone bubbling fluidized beds employed as GSC reactors, there is little doubt that the concept can operate successfully at large scale under pressurized conditions. Lab-scale pressurized experiments have not encountered serious technical challenges [64,65]. The key uncertainty is related to the maximum achievable operating temperature. The oxygen carrier material, reactor body, and downstream valves and filters must all be able to withstand the maximum reactor operating temperature (assumed to be 1200 °C in this study). Lower GSC operating temperatures will reduce the plant efficiency in power mode as more hydrogen needs to be extracted from

Table 2
Gasification island assumptions.

Winkler Gasifier & Pre-gasifier Exchanger		
Item	***Value***	***Units***
Freeboard temperature	900	°C
Gasifier pressure	44	bar
Oxidizer overpressure	400	kPa
Syngas recuperator MITA	30	°C
HP steam superheat	450	°C
Overall Fixed carbon conversion	97	%
Heat loss as %LHV	0.5	%
Coal milling	50	MJ/kg coal
Ash handling	100	MJ/kg ash
Pre-gasifier MITA	30	°C
Fixed carbon conversion in pre-gasifier	~20	%
%w. solids in slurry	65	%
Slurry pump efficiency	80	%
Shell Gasifier		
Item	***Value***	***Units***
Moderator (steam) to dry coal ratio	0.09	kg/kg
Oxygen to dry coal ratio	0.873	kg/kg
Moisture in coal after drying	2	%
Syngas for coal drying %LHV	0.9	%
Fixed carbon conversion	99.3	%
Gasifier operating pressure	44	bar
Steam moderator pressure	54	bar
Heat loss as %LHV	0.7	%
Heat to membrane wall as %LHV	2	%
CO_2 coal loading		
CO_2 HP/HHP pressure	56/88	bar
CO_2 temperature	80	°C
CO_2 to dry coal ratio	0.83	kg/kg
N_2 coal loading		
N_2 HP/HHP pressure	88	bar
N_2 temperature	88	°C
N_2 to dry coal ratio	0.28	kg/kg
HP-ASU		
Main air compressor polytropic efficiency	89	%
Booster air compressor polytropic efficiency	87	%
Reboiler–condenser pinch	1.5	°C
Heat exchanger minimum approach temperature	2	°C
Oxygen purity	95	%
Oxygen delivery pressure	48	bar
Oxygen pump efficiency	80	%
Exchanger pressure losses/side	10	kPa
Intercooler pressure loss	10	kPa
LP-ASU		
Specific O_2 consumption	325	kWh/tonO_2
O_2 delivery pressure	48	bar
N_2 delivery pressure	1.2	bar

Table 3
HGCU modelling assumptions.

HGCU		
Item	***Value***	***Units***
Adsorption temperature	400	°C
Regeneration temperature	750	°C
Filter pressure drop	5	%
Auxiliary consumption	5.34	MJe/kgH_2S
Fresh sorbent ZnO/TiO_2 ratio	1	–
ZnS/ZnO ratio ex regenerator	0.1	–
Compander polytropic efficiency	90	%
Syngas blower polytropic efficiency	89	%
Compander mechanical efficiency	99	%
O_2 mol fraction in regeneration stream	2	%

Table 4
MAWGS reactor modelling assumptions.

MAWGS		
Item	***Value***	***Units***
Membrane heat transfer coefficient	200	W/m^2K
N° of tubes	6000	–
Tube height	10	m
Tube diameter	0.05	m
Retentate side ΔP	200	kPa
Permeate side ΔP	20	kPa
Membrane void fraction	0.5	–
Membrane density	5240	kg/m^3
Maximum membrane temperature	600	°C

the syngas stream and recompressed for injection into the added combustor, and more steam must be extracted from the steam cycle for the WGS reaction.

MAWGS reactor. Pd-based hydrogen perm-selective membranes are an established technology and have been demonstrated for MAWGS reactors [66], but long-term durability along with long-term cost reduction potential remain uncertain. Alternatively, the conventional combination of WGS and PSA can be used, where the shifted syngas must be cooled before producing a pressurized H_2 stream and a low-pressure depleted syngas stream. This option is expected to reduce efficiency for power production because of the poorer integration potential of the heat in the syngas stream and the additional heat released by the WGS reaction. For H_2 production mode, however, conventional WGS and PSA could be attractive because the large H_2 stream is produced at elevated pressure.

Added combustor. Controlled and low-emission spontaneous combustion of hydrogen injected into the hot depleted air stream from the GSC reactors needs to be demonstrated. If multiple fuel injectors are used to evenly distribute the fuel in the oxidant stream, this combustor could achieve low-NOx combustion performance similar to premixed combustors. The present study assumes that such combustion can be completed using pure hydrogen as fuel. If future studies indicate a necessity for fuel dilution, N_2 from the ASU could be used as a sweep gas in the MAWGS reactor to allow for higher membrane permeate pressures, thereby minimizing efficiency losses associated with fuel dilution. From an experimental point of view, high-temperature air combustion has been studied for many years, mainly for application in furnaces. However, high flame stability and pollutant reductions also make it an interesting application for gas turbines [67].

Pre-gasifier. As discussed earlier, the pre-gasifier adds significant gains in efficiency and CO_2 capture ratio and is also expected to considerably reduce plant capital costs. However, it does introduce significant uncertainty. Fouling is likely to be high in the tubes carrying the slurry, although the potential cost increases from a reduced heat transfer coefficient due to fouling should be minimized by a relatively large temperature difference driving heat exchange. The rate of the endothermic gasification reactions must also be high enough so that the ash melting point is not crossed. If this is not possible, more water could be added to the slurry, leading to a minor efficiency penalty but also to less methane formation that will allow more H_2 extraction when the plant is operated in H_2 production mode. Furthermore, the unknown size of the coal particles after slurry water evaporation can significantly affect the gasifier performance, although the flexibility of fluidized bed gasifiers mitigate this risk. Understanding these effects will require separate experimental demonstration activities. Some experimental studies have already been done, showing that it is possible to vaporize the slurry without coal particle agglomeration [68].

System flexibility. Operation as a fully flexible load-following plant could be practically challenging due to the reduction in the gas turbine pressure ratio under part-load operation. This reduced pressure changes the duties of the syngas expander and CO_2 compressor and will also affect the heat transfer characteristics in the recuperator or slurry pre-gasifier. In addition, flexible operation of the bottoming cycle could pose challenges due to the need to supply steam at constant pressure to the gasification section, despite the large change in load between power mode and H_2 production mode. A practically simpler option would be to design the plant for binary power or hydrogen production by including a small added gas turbine for operation only during H_2 production mode with a TIT that can be achieved without added firing and the same pressure ratio as the large H_2-class turbine. In this way, the system pressure remains constant when switching between power and H_2 modes. This turbine can be sized such that remaining heat sources only supply process steam, avoiding challenges with steam cycle integration. The cost of this added turbine should be comparable to the avoided cost of oversizing the syngas expander and CO_2 compressors for part-load operation of the H-class turbine at a lower pressure ratio.

Prior to the development of these technological enablers, an *ex ante* economic assessment should be carried out to weigh the benefits of the novel configurations proposed relative to established, de-risked CCS technologies such as the pre-combustion CO_2 capture IGCC plant

Table 5
Power island modelling assumptions.

Natural gas fired Gas Turbine specs at 9 °C ambient temperature		
Item	***Value***	***Units***
Inlet air flow rate	947.6	kg/s
Pressure Ratio	23.6	-
Rated Power	520	MW
COT_{Ref}	1648	°C
TIT_{Ref}	1550	°C
TOT_{Ref}	641	°C
Simple cycle efficiency	43.0	%
Exhaust pressure loss	3500	Pa
Steam Cycle		
Item	***Value***	***Units***
Condenser pressure	0.04	bar
Auxiliaries for heat rejection	0.008	kW/kW_{th}
Water pumps isentropic efficiency	80	%
LP/IP Pinch point	10	°C
LP/IP Approach point	9	°C
LP ΔP/P eco + eva	25	%
IP ΔP/P eco + eva	15	%
ΔP/P superheaters	8	%
HP pinch (once through)	9	°C
Pressure level in drum (HP/IP/LP)	185/43/6	bar
LP superheat	300	°C
LP Stage isentropic efficiency	87.7	%
IP Stage isentropic efficiency	92.0	%
HP Stage isentropic efficiency	90.3	%
Electromechanical Efficiency	98.3	%
Maximum steam temperature	600	°C
CO_2/H_2 Compression & Syngas Expander/ Heat Recovery		
Item	***Value***	***Units***
CO_2 compression polytropic efficiency	82	%
CO_2 Pump isentropic efficiency	80	%
H_2 compression polytropic efficiency	85	%
Intercooler pressure drop	5–20	kPa
Process streams cooled to	25	°C
Syngas expander polytropic efficiency	87	%
H_2 Recuperator MITA	20	°C
Syngas recuperator MITA	30	°C

Table 6
Douglas Premium coal properties.

Ultimate Analysis	**Mass Frac**
C	0.6652
N	0.0156
H	0.0378
S	0.0052
O	0.0546
Cl	0.00009
Moisture	0.08
Ash	0.1415
Volatiles	0.2291
LHV (MJ/kg)	25.17

presented in this work.

5. Summary and conclusions

In this work, a flexible plant configuration for H_2 and power production based on the integration of a GSC cluster with a MAWGS reactor has been proposed. An advanced scheme with coal water slurry pre-gasification using the high-temperature GSC reduction stage outlet was also developed. Both plants were consistently benchmarked against an unabated IGCC plant and a pre-combustion CO_2 capture IGCC plant utilizing modern gas turbine technology and HGCU for syngas treating. The benefits derived from this technological feature are to a degree limited in the unabated IGCC plant due to the need to extract steam from the bottoming cycle to limit NOx emissions, while in the pre-combustion plant the efficiency gain is reduced due to the ambient temperature CO_2 extraction in the Selexol unit. From an electrical efficiency point of view, the GSC-MAWGS plant with reduction gases recuperator to preheat the syngas routed to the GSC was capable of reducing the energy penalty due to CCS by 5.3%-points relative to the pre-combustion benchmark, while the GSC-MAWGS IGCC plant with slurry pre-gasification achieved an 8.4%-points reduction. Alongside this, the novel plants reached CO_2 avoidance rates up to 8.5%-points above the reference CCS technology.

Besides these attractive performance figures, the proposed configuration can operate to produce H_2 as an energy vector in times of low electricity prices, where the demand is satisfied by existing renewable energy infrastructure. This is done by ramping down the GT to 10% of its rated power and bypassing most of the syngas fuel to the MAWGS reactor, while the traditionally inflexible units (gasification, ASU, etc.) can operate continuously. Low part-load operation of the GT for long

Table 7
Stream data for the unabated IGCC plant.

Property				% mol								
Stream n°	P (bar)	T (°C)	m (kg/s)	N_2	O_2	Ar	CO_2	H_2O	CO	H_2	CH_4	H_2S
1	1.0	25.0	61.0	Douglas Premium Coal								
2	88.0	25.0	16.0	99.9	0.0	0.1	0.0	0.0	0.0	0.0	0.0	0.0
3	48.0	180.0	51.7	2.1	95.0	2.9	0.0	0.0	0.0	0.0	0.0	0.0
4	1.0	15.0	114.0	77.3	20.7	0.9	0.0	1.0	0.0	0.0	0.0	0.0
5	23.9	455.8	114.0	77.3	20.7	0.9	0.0	1.0	0.0	0.0	0.0	0.0
6	35.0	187.4	137.9	97.6	2.0	0.5	0.0	0.0	0.0	0.0	0.0	0.0
7	35.0	187.4	137.9	97.6	2.0	0.5	0.0	0.0	0.0	0.0	0.0	0.0
8	44.0	900.0	237.0	5.2	0.0	0.9	2.5	2.7	62.6	25.8	0.2	0.2
9	148.0	450.0	132.5	0.0	0.0	0.0	0.0	100.0	0.0	0.0	0.0	0.0
10	42.0	356.4	112.3	6.2	0.0	0.9	2.5	2.6	61.9	25.5	0.2	0.2
11	39.9	400.0	112.2	6.2	0.0	0.9	2.5	2.8	61.9	25.5	0.2	0.0
12	35.0	312.2	277.5	43.8	0.8	0.6	1.1	14.9	27.4	11.3	0.1	0.0
13	1.0	9.0	833.6	77.3	20.7	0.9	0.0	1.0	0.0	0.0	0.0	0.0
14	23.7	455.8	530.9	77.3	20.7	0.9	0.0	1.0	0.0	0.0	0.0	0.0
15	23.0	1577.8	808.5	69.6	6.0	0.9	12.0	11.7	0.0	0.0	0.0	0.0
16	1.0	641.0	997.3	71.1	8.7	0.9	9.7	9.5	0.0	0.0	0.0	0.0
17	1.0	641.0	997.3	71.1	8.7	0.9	9.7	9.5	0.0	0.0	0.0	0.0
18	41.9	405.1	28.7	0.0	0.0	0.0	0.0	100.0	0.0	0.0	0.0	0.0
19	51.8	300.0	7.1	0.0	0.0	0.0	0.0	100.0	0.0	0.0	0.0	0.0
20	141.8	600.0	219.0	0.0	0.0	0.0	0.0	100.0	0.0	0.0	0.0	0.0
21	39.6	600.0	197.4	0.0	0.0	0.0	0.0	100.0	0.0	0.0	0.0	0.0
22	0.04	29.0	199.5	0.0	0.0	0.0	0.0	100.0	0.0	0.0	0.0	0.0

Table 8
Stream data for the pre-combustion CO_2 capture IGCC plant.

Property				% mol								
Stream n°	P (bar)	T (°C)	m (kg/s)	N_2	O_2	Ar	CO_2	H_2O	CO	H_2	CH_4	H_2S
1	1.0	25.0	71.3	Douglas Premium Coal								
2	88.0	80.0	18.7	99.9	0.0	0.1	0.0	0.0	0.0	0.0	0.0	0.0
3	48.0	22.0	604.5	2.2	95.1	2.9	0.0	0.0	0.0	0.0	0.0	0.0
4	1.0	15.0	133.6	77.3	20.7	0.9	0.0	1.0	0.0	0.0	0.0	0.0
5	23.9	455.8	133.6	77.3	20.7	0.9	0.0	1.0	0.0	0.0	0.0	0.0
6	2.7	22.2	24.3	97.5	2.0	0.5	0.0	0.0	0.0	0.0	0.0	0.0
7	35.0	187.4	161.9	97.5	2.0	0.5	0.0	0.0	0.0	0.0	0.0	0.0
8	44.0	900.0	278.1	5.2	0.0	0.9	2.5	2.7	62.6	25.7	0.2	0.2
9	42.0	356.8	131.4	6.2	0.0	0.9	2.5	2.7	61.9	25.5	0.2	0.2
10	39.9	400.0	131.2	6.2	0.0	0.9	2.5	2.9	61.9	25.5	0.2	0.0
11	37.5	25.0	193.9	3.9	0.0	0.6	39.9	0.1	0.7	54.7	0.1	0.0
12	36.5	25.0	35.2	6.3	0.0	0.9	3.9	0.0	1.2	87.5	0.2	0.0
13	35.0	220.0	224.0	45.5	0.9	0.6	1.7	11.4	0.5	39.3	0.1	0.0
14	1.0	9.0	837.5	77.3	20.7	0.9	0.0	1.0	0.0	0.0	0.0	0.0
15	23.7	455.8	481.9	77.3	20.7	0.9	0.0	1.0	0.0	0.0	0.0	0.0
16	23.0	1650.7	705.8	69.4	3.4	0.9	1.2	25.1	0.0	0.0	0.0	0.0
17	1.0	641.0	928.7	71.1	7.3	0.9	0.9	19.8	0.0	0.0	0.0	0.0
18	1.0	98.4	928.7	71.1	7.3	0.9	0.9	19.8	0.0	0.0	0.0	0.0
19	150.0	25.0	158.2	0.2	0.0	0.0	99.7	0.0	0.0	0.2	0.0	0.0
20	141.8	600.0	277.5	0.0	0.0	0.0	0.0	100.0	0.0	0.0	0.0	0.0
21	148.1	450.0	155.5	0.0	0.0	0.0	0.0	100.0	0.0	0.0	0.0	0.0
22	154.9	351.5	82.9	0.0	0.0	0.0	0.0	100.0	0.0	0.0	0.0	0.0
23	41.9	405.1	103.5	0.0	0.0	0.0	0.0	100.0	0.0	0.0	0.0	0.0
24	43.0	255.7	22.2	0.0	0.0	0.0	0.0	100.0	0.0	0.0	0.0	0.0
25	51.8	300.0	8.3	0.0	0.0	0.0	0.0	100.0	0.0	0.0	0.0	0.0
26	39.6	600.0	182.3	0.0	0.0	0.0	0.0	100.0	0.0	0.0	0.0	0.0
27	0.04	29.0	203.9	0.0	0.0	0.0	0.0	100.0	0.0	0.0	0.0	0.0

periods is acceptable as harmful emissions are avoided due to the flameless combustion taking place in the GSC, therefore allowing a higher degree of flexibility output between power and H_2. The equivalent H_2 production efficiency is in line with the values reached in pre-combustion H_2 production IGCC plants designed for low electricity outputs [55] for the GSC-MAWGS IGCC plant with the reduction gases recuperator (56.6%), but increase substantially to 62.5% for the pre-gasification case. This is achieved because the reduction gases of the GSC effectively transfer sensible heat to the gasification feed, minimizing the oxidant requirements from the ASU. In this case, the gross electricity output of the combined cycle matched the auxiliary consumption demand of the plant.

In conclusion, the present work outlines two efficient IGCC schemes with CCS, using a modern H-class GT, which overcome the inflexibility feature of traditional IGCC 'baseload' power plants by using H_2 as an energy storage vector. Such a plant can simultaneously balance variable renewables and produce cost-effective hydrogen for decarbonizing other sectors like industry, transport, and heat. To realize this promising performance, further development and demonstration efforts are required for GSC and MAWGS reactors, the added combustor, and the

Table 9
Stream data for the GSC-MAWGS IGCC plant with reduction gases recuperator.

Property				**% mol**								
Stream n°	P (bar)	T (°C)	m (kg/s)	N_2	O_2	Ar	CO_2	H_2O	CO	H_2	CH_4	H_2S
1	1.0	25.0	59.1	Douglas Premium Coal								
2	48.0	22.1	50.1	1.1	95.0	3.9	0.0	0.0	0.0	0.0	0.0	0.0
3	1.0	15.0	205.1	77.3	20.7	0.9	0.0	1.0	0.0	0.0	0.0	0.0
4	1.2	22.1	135.4	99.9	0.0	0.1	0.0	0.0	0.0	0.0	0.0	0.0
5	1.2	22.1	18.2	99.9	0.0	0.1	0.0	0.0	0.0	0.0	0.0	0.0
6	44.0	900.0	224.0	1.1	0.0	1.3	6.4	4.6	63.1	23.1	0.1	0.2
7	154.1	450.0	119.9	0.0	0.0	0.0	0.0	100.0	0.0	0.0	0.0	0.0
8	42.0	388.5	118.9	1.1	0.0	1.3	7.3	4.5	62.4	22.9	0.1	0.2
9	39.9	400.0	117.4	1.1	0.0	1.3	7.3	4.7	62.4	22.9	0.1	0.0
10	39.9	400.0	48.1	1.1	0.0	1.3	7.3	4.7	62.4	22.9	0.1	0.0
11	39.9	323.0	131.5	0.5	0.0	0.6	3.4	55.5	29.2	10.7	0.1	0.0
12	37.9	599.9	127.2	0.8	0.0	0.9	45.6	42.3	3.1	7.1	0.1	0.0
13	23.1	1102.0	175.2	0.9	0.0	1.0	1.0	33.1	30.1	22.5	12.3	0.0
14	22.4	592.8	212.2	1.6	0.1	1.0	55.1	42.1	0.0	0.0	0.0	0.0
15	22.1	25.0	50.2	0.0	0.0	0.0	1.0	99.0	0.0	0.0	0.0	0.0
16	150.0	25.0	140.8	2.7	0.2	1.8	95.3	0.0	0.0	0.0	0.0	0.0
17	88.0	80.0	41.2	2.7	0.2	1.8	95.3	0.0	0.0	0.0	0.0	0.0
18	2.6	598.6	4.3	0.0	0.0	0.0	0.0	0.0	0.0	100.0	0.0	0.0
19	35.0	578.6	4.3	0.0	0.0	0.0	0.0	0.0	0.0	100.0	0.0	0.0
20	1.0	9.0	947.6	77.3	20.7	0.9	0.0	1.0	0.0	0.0	0.0	0.0
21	23.1	450.3	765.4	77.3	20.7	0.9	0.0	1.0	0.0	0.0	0.0	0.0
22	22.6	1130.0	728.4	80.7	17.2	1.0	0.1	1.1	0.0	0.0	0.0	0.0
23	21.9	1648.2	732.8	77.4	12.4	0.9	0.1	9.1	0.0	0.0	0.0	0.0
24	1.0	630.7	915.1	77.4	14.0	0.9	0.1	7.6	0.0	0.0	0.0	0.0
25	1.0	126.7	915.1	77.4	14.0	0.9	0.1	7.6	0.0	0.0	0.0	0.0
26	41.9	405.1	53.6	0.0	0.0	0.0	0.0	100.0	0.0	0.0	0.0	0.0
27	43.0	255.7	8.6	0.0	0.0	0.0	0.0	100.0	0.0	0.0	0.0	0.0
28	141.8	600.0	227.0	0.0	0.0	0.0	0.0	100.0	0.0	0.0	0.0	0.0
29	39.6	600.0	182.1	0.0	0.0	0.0	0.0	100.0	0.0	0.0	0.0	0.0
30	0.04	29.0	197.0	0.0	0.0	0.0	0.0	100.0	0.0	0.0	0.0	0.0

Table 10
Stream data of the GSC-MAWGS IGCC plant with slurry pre-gasifier.

Property				**% mol**								
Stream n°	P (bar)	T (°C)	m (kg/s)	N_2	O_2	Ar	CO_2	H_2O	CO	H_2	CH_4	H_2S
1	1.0	25.0	48.6	Douglas Premium Coal								
2	1.0	60.0	26.2	0.0	0.0	0.0	0.0	100.0	0.0	0.0	0.0	0.0
3	1.0	15.0	71.0	77.3	20.7	0.9	0.0	1.0	0.0	0.0	0.0	0.0
4	48.0	22.1	17.3	1.1	95.0	3.9	0.0	0.0	0.0	0.0	0.0	0.0
5	1.2	22.1	38.2	99.9	0.0	0.1	0.0	0.0	0.0	0.0	0.0	0.0
6	1.2	22.1	14.9	99.9	0.0	0.1	0.0	0.0	0.0	0.0	0.0	0.0
7	44.0	900.0	84.5	0.7	0.0	0.5	6.9	5.4	43.0	36.0	7.3	0.2
8	39.9	400.0	84.3	0.7	0.0	0.5	6.9	5.6	43.0	36.0	7.3	0.0
9	39.9	400.0	31.1	0.7	0.0	0.5	6.9	5.6	43.0	36.0	7.3	0.0
10	39.9	372.0	92.9	0.4	0.0	0.3	3.9	46.4	24.4	20.4	4.2	0.0
11	37.9	599.8	88.8	0.7	0.0	0.4	44.4	39.1	2.6	5.8	6.9	0.0
12	22.9	797.0	119.9	0.7	0.0	0.4	31.1	27.2	17.0	16.5	7.0	0.0
13	22.4	1118.0	166.7	1.3	0.1	0.4	47.9	50.3	0.0	0.0	0.0	0.0
14	22.0	25.0	50.3	0.0	0.0	0.0	1.0	99.0	0.0	0.0	0.0	0.0
15	150.0	25.0	116.3	2.5	0.3	0.8	96.4	0.0	0.0	0.0	0.0	0.0
16	2.2	599.6	4.1	0.0	0.0	0.0	0.0	0.0	0.0	100.0	0.0	0.0
17	2.2	579.6	4.1	0.0	0.0	0.0	0.0	0.0	0.0	100.0	0.0	0.0
18	1.0	9.0	947.6	77.3	20.7	0.9	0.0	1.0	0.0	0.0	0.0	0.0
19	22.9	447.9	767.5	77.3	20.7	0.9	0.0	1.0	0.0	0.0	0.0	0.0
20	22.4	1153.0	720.8	81.7	16.1	1.0	0.1	1.2	0.0	0.0	0.0	0.0
21	21.7	1647.8	724.9	78.5	11.6	0.9	0.1	8.9	0.0	0.0	0.0	0.0
22	1.0	632.2	906.1	78.3	13.3	0.9	0.1	7.4	0.0	0.0	0.0	0.0
23	1.0	127.7	906.1	78.3	13.3	0.9	0.1	7.4	0.0	0.0	0.0	0.0
24	43.0	255.7	2.3	0.0	0.0	0.0	0.0	100.0	0.0	0.0	0.0	0.0
25	41.9	405.1	37.4	0.0	0.0	0.0	0.0	100.0	0.0	0.0	0.0	0.0
26	148.0	450.0	13.1	0.0	0.0	0.0	0.0	100.0	0.0	0.0	0.0	0.0
27	43.0	360.0	7.1	0.0	0.0	0.0	0.0	100.0	0.0	0.0	0.0	0.0
28	141.8	600.0	133.9	0.0	0.0	0.0	0.0	100.0	0.0	0.0	0.0	0.0
29	39.6	600.0	103.5	0.0	0.0	0.0	0.0	100.0	0.0	0.0	0.0	0.0
30	0.0	29.0	136.0	0.0	0.0	0.0	0.0	100.0	0.0	0.0	0.0	0.0

slurry pre-gasifier. As future work, a rigorous economic and system integration study should be completed to quantify the potential reductions in total energy system costs and emissions that can be realized by this flexible plant.

CRediT authorship contribution statement

Carlos Arnaiz del Pozo: Methodology, Formal analysis, Investigation, Writing - original draft. **Schalk Cloete:** Conceptualization, Methodology, Writing - original draft, Supervision, Funding acquisition. **Paolo Chiesa:** Formal analysis, Writing - original draft. **Ángel Jiménez Álvaro:** Formal analysis, Writing - review & editing, Supervision, Funding acquisition. **Shahriar Amini:** Writing - review & editing, Project administration, Funding acquisition.

Declaration of Competing Interest

The authors declare that they have no known competing financial interests or personal relationships that could have appeared to influence the work reported in this paper.

Acknowledgements

This research received financial support from the ERA-NET cofund, ACT GaSTech Project number 276321 co-funded by the European Commission under the Horizon 2020 program, and ACT Grant Agreement No. 691712. The partners collaborating in this article have received funding from Ministerio de Economía y Competitividad (MINECO), Spain (reference PCIN-2017-013) and the Research Council of Norway, Norway. The authors would also like to acknowledge Honeywell for the free Academic License of Unisim Design Suite R451 and CO-LaN for the Academic CAPE-OPEN license.

A. Appendix

Tables 2-10.

References

[1] Anonymous “European, Geosciences Union's Reaction to IPCC Report on Global Warming of 1.5 Degrees Celsius” Targeted News Service; 2018.
[2] Anonymous “Global CCS Institute: Targeting Climate Change ” Targeted News Service; 2019.
[3] N.A. Sepulveda, J.D. Jenkins, F. de Sisternes J. and R.K. Lester, “The Role of Firm Low-Carbon Electricity Resources in Deep Decarbonization of Power Generation” Joule; 2018, vol. 2, no. 11, pp. 2403-2420.
[4] Ishida, M., Zheng, D., Akehata, T., “Evaluation of a chemical-looping-combustion power-generation system by graphic exergy analysis. ” Energy. 1987, pp. 12, 147-154.
[5] Zhu L, He Y, Li L, Wu P. Tech-economic assessment of second-generation CCS: Chemical looping combustion. Energy. 2018;144:915–27.
[6] Jiménez Álvaro Á, López Paniagua I, González Fernández C, Rodríguez Martín J, Nieto Carlier R. Simulation of an integrated gasification combined cycle with chemical-looping combustion and carbon dioxide sequestration. Energy Convers Manage 2015;104:170–9.
[7] Mattisson T, Keller M, Linderholm C, Moldenhauer P, Rydén M, Leion H, et al. Chemical-looping technologies using circulating fluidized bed systems: Status of development. Fuel Process Technol. 2018;172:1–12.
[8] Zaabout A, Cloete S, Johansen ST, Van SA, Gallucci F, Amini S. Experimental demonstration of a novel gas switching combustion reactor for power production with integrated CO 2 capture. Ind Eng Chem Res 2013;52(39):14241–50.
[9] Cloete S, Romano MC, Chiesa P, Lozza G, Amini S. Integration of a Gas Switching Combustion (GSC) system in integrated gasification combined cycles. Int J Greenhouse Gas Control 2015;42:340–56.
[10] Zerobin F, Pröll T. Potential and limitations of power generation via chemical looping combustion of gaseous fuels. Int J Greenhouse Gas Control 2017;64:174–82.
[11] Hamers HP, Romano MC, Spallina V, Chiesa P, Gallucci F, Annaland MvS. Comparison on process efficiency for CLC of syngas operated in packed bed and fluidized bed reactors. Int J Greenhouse Gas Control 2014;28:65–78.
[12] Spallina V, Romano MC, Chiesa P, Gallucci F, van SA, Lozza G. Integration of coal gasification and packed bed CLC for high efficiency and near-zero emission power generation. Int J Greenhouse Gas Control 2014;vol:27.
[13] Arnaiz del Pozo C, Cloete S, Cloete JH, Jiménez Álvaro Á, Amini S. The potential of chemical looping combustion using the gas switching concept to eliminate the energy penalty of CO2 capture. Int J Greenhouse Gas Control 2019;83:265–81.
[14] Ito E, Tsukagoshi K, Masada J, Ishazaka K, Saitoh K, Torigoe T., “Key technologies for ultra-high temperature gas turbines. ” Mitsubishi Heavy Industries Tech Rev 2015;52.
[15] Tumanovskii A, Shvarts A, Somova E, Verbovetskii E, Avrutskii G, Ermakova S, et al. Review of the coal-fired, over-supercritical and ultra-supercritical steam power plants. Therm Eng 2017;64(2):83–96.
[16] Research & Develoment Solutions LLC, National Energy Technology Laboratory, “Cost Performance Baseline for power plants study: Volume 1 - Bituminous coal and natural gas to electricty” 2007.
[17] Giuffrida A, Romano M, Lozza G. Thermodynamic Assessment of IGCC Plants with Hot Gas Desulphurization. Appl Energy 2010;87(11):3374–83.
[18] Liu D, Wang Q, Wu J, Liu Y. A review of sorbents for high-temperature hydrogen sulfide removal from hot coal gas. Environ Chem Lett 2019;17(1):259–76.
[19] Hirth L, Ueckerdt F, Edenhofer O. Integration costs revisited – An economic framework for wind and solar variability. Renewable Energy 2015;74:925–39.
[20] Hirth L. The Optimal Share of Variable Renewables: How the Variability of Wind and Solar Power affects their Welfare-optimal Deployment. Energy J 2015;36(1):1.
[21] Dowella N, Staffella I. The role of flexible CCS in the UK's future energy system. Int J Greenhouse Gas Control 2016;48:327–44.
[22] Cloete S, Hirth L. Flexible power and hydrogen production: Finding synergy between CCS and variable renewables. Energy 2020;vol:192.
[23] R. Anantharaman, O. Bolland, N. Booth, E. Van Dorst, E. Sanchez Fernandez, F. Franco, E. Macchi, G. Manzolini, D. Nikolic, A. Pfeffer, M. Prins, S. Rezvani and L. Robinson, “Cesar Deliverable D2.4.3. European Best Practice Guidelines For Assessment Of Co2 Capture Technologies”; 2018.
[24] Gazzani M, Macchi E, Manzolini G. CO2 capture in integrated gasification combined cycle with SEWGS – Part A: Thermodynamic performances. Fuel 2013;105:206–19.
[25] Uemiya S, Sato N, Ando H, Kikuchi E. The water gas shift reaction assisted by a palladium membrane reactor. Ind Eng Chem Res 1991;30(3):585–9.
[26] Gallucci F, Fernandez E, Corengia P, van Sint Annaland M. Recent advances on membranes and membrane reactors for hydrogen production. Chem Eng Sci 2013;92:40–66.
[27] Ozcan H, Dincer I. Thermodynamic analysis of a combined chemical looping-based trigeneration system. Energy Convers Manage 2014;85:477–87.
[28] Toporov D, Abraham R. Gasification of low-rank coal in the High-Temperature Winkler (HTW) process. J South Afr Inst Min Metall 2015;115(7):589–97.
[29] Unisim Design Suite, “https://www.honeywellprocess.com/library/marketing/notes/unisimdesign-pin-r451.pdf”.
[30] Scilab, “https://www.scilab.org/”.
[31] Hla SS, Park D, Duffy GJ, Edwards JH, Roberts DG, Ilyushechkin A, et al. Kinetics of high-temperature water-gas shift reaction over two iron-based commercial catalysts using simulated coal-derived syngases. Chem Eng J 2009;146(1):148–54.
[32] Fernandez E, Medrano JA, Melendez J, Parco M, Viviente JL, van Sint Annaland M, et al. Preparation and characterization of metallic supported thin Pd–Ag membranes for hydrogen separation. Chem Eng J 2016;305:182–90.
[33] Romano MC, Chiesa P, Lozza G. Pre-combustion CO2 capture from natural gas power plants, with ATR and MDEA processes. Int J Greenhouse Gas Control 2010;4(5):785–97.
[34] Moioli S, Giuffrida A, Romano MC, Pellegrini LA, Lozza G. Assessment of MDEA absorption process for sequential H2S removal and CO2 capture in air-blown IGCC plants. Appl Energy 2016;183:1452–70.
[35] R.A. Robie and B.S. Hemingway, “Thermodynamic properties of minerals and related substances at 298.15 K and 1 bar (105 Pascals) pressure and at higher temperatures”; 1995.
[36] P.J. Linstrom and W.G. Mallard, “NIST Chemistry WebBook, NIST Standard Reference Database Number 69”; 2020.
[37] Cloete S, Zaabout A, Romano MC, Chiesa P, Lozza G, Gallucci F, et al. Optimization of a Gas Switching Combustion process through advanced heat management strategies. Appl. Energy. 2017;185:1459–70.
[38] Abad A, Adánez J, García-Labiano F, de Diego L, Gayán FP, Celaya J. Mapping of the range of operational conditions for Cu-, Fe-, and Ni-based oxygen carriers in chemical-looping combustion. Chem Eng Sci 2007;62(1–2):533–49.
[39] Fan J, Hong H, Zhu L, Wang Z, Jin H. Thermodynamic evaluation of chemical looping combustion for combined cooling heating and power production driven by coal. Energy Convers Manage 2017;135:200–11.
[40] Kuusik R, Trikkel A, Lyngfelt A, Mattisson T. High temperature behavior of NiO-based oxygen carriers for Chemical Looping Combustion. Energy Procedia 2009;1(1):3885–92.

[41] Yonamine W, Thangavel S, Ohashi H, Fushimi C. Performance analysis of a water–gas shift membrane reactor for integrated coal gasification combined cycle plant. Energy Convers Manage 2018;174:552–64.
[42] Amelio M, Morrone P, Gallucci F, Basile A. Integrated gasification gas combined cycle plant with membrane reactors: Technological and economical analysis. Energy Convers Manage 2007;48(10):2680–93.
[43] Lin Y, Rei M. Study on the hydrogen production from methanol steam reforming in supported palladium membrane reactor. Catal Today 2001;67(1–3):77–84.
[44] Basile A, Gallucci F, Paturzo L. A dense Pd/Ag membrane reactor for methanol steam reforming: experimental study. Catal Today 2005;104(2–4):244–50.
[45] Jones D, Bhattacharyya D, Turton R, Zitney SE. Optimal design and integration of an air separation unit (ASU) for an integrated gasification combined cycle (IGCC) power plant with CO 2 capture. Fuel Process Technol. 2011;92(9):1685–95.
[46] S. Martini, M. Kleinhappl and H. Hofbauer, “High temperature gas treatment for clean gas applications”, 2010.
[47] Ohtsuka Y, Tsubouchi N, Kikuchi T, Hashimoto H. Recent progress in Japan on hot gas cleanup of hydrogen chloride, hydrogen sulfide and ammonia in coal-derived fuel gas. Powder Technol. 2009;190(3):340–7.
[48] Giuffrida A, Romano MC, Lozza G. Efficiency enhancement in IGCC power plants with air-blown gasification and hot gas clean-up. Energy. 2013;53:221–9.
[49] Chiesa P, Lozza G, Mazzocchi L. Using Hydrogen as Gas Turbine Fuel. Journal of Engineering for Gas Turbines and Power (Transactions of the ASME). 2005;127(1):73–80.
[50] M. Gazzani, P. Chiesa, E. Martelli, S. Sigali and I. Brunetti, “Using Hydrogen as Gas Turbine Fuel: Premixed Versus Diffusive Flame Combustors” J Eng Gas Turbines Power. Trans ASME; 2014, vol. 136, no. 5, pp. np.
[51] S.C. Gülen, “Gas Turbines for Electric Power Generation”; 2019.
[52] Jansen D, Gazzani M, Manzolini G, Dijk Ev, Carbo M. Pre-combustion CO2 capture. Int J Greenhouse Gas Control 2015;40:167–87.
[53] Arnaiz dP, Cloete S, Hendrik Cloete J, Jiménez Álvaro Á, Amini S. The oxygen production pre-combustion (OPPC) IGCC plant for efficient power production with CO 2 capture. Energy Convers Manage 2019;vol:201.
[54] Davison J. Electricity systems with near-zero emissions of CO 2 based on wind energy and coal gasification with CCS and hydrogen storage. Int J Greenhouse Gas Control 2009;3(6):683–92.
[55] Davison J, Mancuso L, Ferrari N. Costs of CO2 Capture Technologies in Coal Fired Power and Hydrogen Plants. Energy Procedia 2014;63:7598–607.
[56] J. Acquaviva, S. Hopkins, “High-performance, durable, palladium alloy membrane for hydrogen separation and purification” Pall Corporation; 2009.
[57] Cloete S, Tobiesen A, Morud J, Romano M, Chiesa P, Giuffrida A, et al. Economic assessment of chemical looping oxygen production and chemical looping combustion in integrated gasification combined cycles. Int J Greenhouse Gas Control 2018;78:354–63.
[58] Zhang X, Keramati H, Arie M, Singer F, Tiwari R, Shooshtari A, et al. “Recent developments in high temperature heat exchangers: A review. Front Heat Mass Transfer 2018;11:11.
[59] M. Sankir and N. Demirci Sankir, “Hydrogen production technologies”; 2017.
[60] M. Wechsung, A. Feldmüller and H. Lemmen, “Steam Turbines for Flexible Load Operation in the Future Market of Power Generation”; 2012, pp. 579-588.
[61] C. Higman, “Gasification” 2nd ed.; 2008.
[62] N. Hack, S.Unz, M. Bechmann, “High temperature ceramic heat exchanger for heat recovery in coal and biomass gasification processes”; 2014.
[63] Bottino A, Comite A, Capannelli G, Di Felice R, Pinacci P. Steam reforming of methane in equilibrium membrane reactors for integration in power cycles. Catal Today 2006;118(1):214–22.
[64] Zaabout A, Cloete S, Amini S. Autothermal operation of a pressurized Gas Switching Combustion with ilmenite ore. Int J Greenhouse Gas Control 2017;63:175–83.
[65] Zaabout A, Cloete S, Tolchard JR, Amini S. A pressurized Gas Switching Combustion reactor: Autothermal operation with a CaMnO3â’ Î-based oxygen carrier. Chem Eng Res Design 2018;137:20–32.
[66] Catalano J, Guazzone F, Mardilovich IP, Kazantzis NK, Ma YH. Hydrogen production in a large scale waterâ€“gas shift Pd-based catalytic membrane reactor. Ind Eng Chem Res 2013;52(3):1042–55.
[67] H. Tsuji, A.K. Gupta, T. Hasegawa, M. Katsuki, K. Kishimoto and M. Morita, “High temperature air combustion: from energy conservation to pollution reduction”; 2002.
[68] Aiuchi K, Moriyama R, Takeda S, Kitada S, Onozaki M, Katayama Y. A pre-heating vaporization technology of coal-water-slurry for the gasification process. Fuel Process Technol 2007;88(4):325–31.